Master Thesis
TVVR24/5004

Modelling the effect of sediment and solid waste deposition on urban flooding in Kampala, Uganda

Hjalmar Olsson

Division of Water Resources Engineering
Department of Building and Environmental Technology
Lund University

Modelling the effect of sediment and solid waste deposition on urban flooding in Kampala, Uganda

By:
Hjalmar Olsson

Master Thesis

Division of Water Resources Engineering
Department of Building & Environmental Technology
Lund University
Box 118
221 00 Lund, Sweden

Water Resources Engineering
TVVR24/5004
ISSN 1101-9824

Lund 2024
www.tvrl.lth.se

Master Thesis
Division of Water Resources Engineering
Department of Building & Environmental Technology
Lund University

English title:	Modelling the effect of sediment and solid waste deposition on urban flooding in Kampala, Uganda
Author(s):	Hjalmar Olsson
Supervisor:	Johanna Sörensen and Seith Mugume
Examiner:	Magnus Larson
Language	English
Year:	2024
Keywords:	Sediment deposition; Solid waste deposition; Pluvial flooding; Kampala; Flood risk management; PCSWMM; Hydraulic modeling; Climate change; Urban drainage systems (UDS)

Acknowledgements

I would like to express my sincere gratitude to all those who have supported and guided me throughout the course of this master thesis project.

Firstly, I am deeply grateful to my supervisors, Johanna Sörensen and Seith Mugume, for their invaluable guidance and constant encouragement. I am particularly grateful for their openness and willingness to answer my questions at any time, which has been crucial in shaping this work.

I extend my thanks to my examinator, Magnus Larson for his constructive feedback and valuable suggestions during this project, which significantly improved the quality of my work.

Special thanks to Philip Tumwine, Otto Raphael, Dorothy Adeke, Keith Bwowe, Martina Namakula, and Ebbe Jansson for their support and collaboration throughout my research.

I would like to extend my sincere appreciation to the Division of Water Resources Engineering and the Department of Building and Environmental Technology at Lund University and Makerere University in Kampala for their collaboration and support during my project.

I also wish to thank EnviDan for providing a computer, which was essential in carrying out my research.

To Åforsk, Miljöfonden, and Sveriges Ingenjörer, I am profoundly grateful for the scholarships provided. Without your financial support, I would not have been able to undertake and complete this project.

To my family and friends, thank you for your unwavering support, encouragement, and understanding during the demanding times of this project.

Lastly, I want to thank my girlfriend, Valentina Pincerato-Hedvall, for always supporting me and being there. Ti amo.

Hjalmar Olsson

Abstract

Pluvial flooding is a significant and growing issue in Kampala, Uganda, driven by increased urbanization, lack of sufficient maintenance of the urban drainage system and climate change. This study investigates the impact of sediment and solid waste deposition on urban flooding within the upstream part of the Lubigi catchment area. Using PCSWMM, a 1D hydraulic model was developed to simulate various scenarios of sediment and solid waste deposition in combination with extreme rainfall events. Field observations, including high-resolution rain data and water level measurements, were implemented, and used for model calibration and validation. The study reveals three critical points vulnerable to flooding in the upstream Lubigi catchment area considering current sediment and solid waste deposition. Furthermore, the results show that increasing sediment and solid waste deposition significantly increases the flooded volume, not only for high return periods but also for lower return periods. In addition, field observations of rainfall suggest that existing synthetic design storms for Kampala may inaccurately estimate the timing of the rainfall peaks. The findings highlight that frequently clearing sediment and solid waste is crucial to mitigating flooding in the upstream Lubigi catchment area.

Keywords: Sediment deposition; Solid waste deposition; Pluvial flooding; Kampala; Flood risk management; PCSWMM; Hydraulic modelling; Climate change; Urban drainage systems (UDSs)

Sammanfattning

Pluviala översvämningar är ett betydande och växande problem i Kampala, Uganda, drivet av ökad urbanisering, otillräckligt underhåll av det urbana avloppssystemet och klimatförändringar. Denna studie undersöker effekterna av sediment- och avfallsackumulering för urbana översvämningar uppströms av Lubigi avrinningsområde. Med hjälp av PCSWMM utvecklades en 1D hydraulisk modell för att simulera olika scenarier av sediment- och avfallsackumulering i kombination med extrema regnhändelser. Fältobservationer, inklusive högupplöst regndata och vattennivåmätningar, implementerades och användes för modellkalibrering och validering. Studien identifierar tre kritiska punkter med avseende på nuvarande sediment- och avfallsackumulering. Vidare visar resultaten att ökande sediment- och avfallsackumulering ökar översvämningsvolymen, inte bara för höga återkomsttider utan även för lägre. Dessutom, antyder fältobservationer av regn att befintliga syntetiska regn för Kampala kan felaktigt uppskatta tidpunkten för regnens toppar. Studien uppmuntrar till att regelbunden borttagning av sediment och avfall är avgörande för att minska översvämningar uppströms Lubigi avrinningsområde.

Nyckelord: Sediment; Avfall; Urbana översvämningar; Kampala; PCSWMM; Hydraulisk modellering; Klimatförändringar; Dagvattensystem

Table of contents

1. Background 1
1.1 Introduction 1
1.2 Problem description 2
1.3 Main objective and research questions 3
2. Theory 4
2.1 Urban drainage 4
2.1.1 Stormwater 5
2.1.2 Flood control 5
2.1.3 Backwater effect 6
2.1.4 Wastewater 7
2.1.5 Sediment and solid waste 7
2.2 Rainfall 8
2.2.1 IDF curves 9
2.2.2 Annual Maximum Method 10
2.2.3 Design storms 10
3. Materials and Methods 11
3.1 Upstream Lubigi catchment area 11
3.2 Methods 13
3.3 Experiment design and scenario description 15
3.4 Tipping Bucket Rain Gauge 16
3.4.1 Calibration of Tipping Bucket Rain Gauge 17
3.4.2 Observed rainfall 19
3.5 Water Level Observations 19
3.6 The Model 22
3.6.1 Extreme Rainfall Analysis 26
3.6.2 Sensitivity analysis 27
3.6.3 Calibration 27
3.6.4 Validation 28

4. Results 29
4.1 Model performance 29
4.2 Critical points vulnerable to flooding 32
4.2.1 Bwaise 33
4.2.2 Alice Kaggwa Road and Kamwokya Kisalosalo Road 37
4.3 Scenario analysis 40
5. Discussion 42
5.1 Model performance 42
5.2 Critical points vulnerable to flooding 43
5.2.1 Bwaise 43
5.2.2 Alice Kaggwa Road and Kamwokya Kisalosalo Road 43
5.3 Scenario Analysis 44
5.4 Rainfall analysis 46
6. Conclusions and Recommendations 47
6.1 Conclusions 47
6.2 Recommendations 48
References 49

1. Background

1.1 Introduction

The world's population is projected to increase in the following decades and Sub-Saharan Africa is projected to be the fastest-growing region until 2050 (UN, 2022). Today more than half of the world's population lives in urban areas, and urbanization is considered to increase even further in the coming decades (UN, 2018). As a result, cities are becoming larger, resulting in more impervious surfaces, causing more frequent flooding events (Sohn et al., 2020; Lawhon et al., 2014). Approximately two-thirds of the urban population growth in Africa is anticipated to result from natural population increase, while the remaining one-third is expected to come from net rural-to-urban migration (UN, 2015).

Compounding the challenges of urban growth, recent studies (Owusu & Oteng-Ababio, 2015; Møller-Jensen et al., 2023; IPCC, 2023) suggests that global climate change will likely increase hydro-climatic disasters, such as urban flooding. The IPCC's Special Report on global warming of 1.5°C above preindustrial levels predicts an increase in flood frequency and magnitude due to changing precipitation patterns (IPCC, 2018). Despite uncertainties in the impacts of climate change on water-related events, frequent extreme rainfall will threaten urban resilience in developing countries due to their low adaptive capacity (IPCC, 2007).

Urban flooding can be characterized in different types. Pluvial flooding occurs when runoff from heavy rainfall exceeds the urban drainage capacity of the system (Maksimović et al., 2009). The increasing frequency and intensity of high-intensity rainfall events, possibly aggravated by climate change, enhance the risk and impact of pluvial flooding (Falconer et al., 2009). Sediment deposition and solid waste accumulation in drainage systems can significantly reduce the capacity to manage runoff, exacerbating pluvial flooding risks. Effective waste management and regular maintenance of drainage infrastructure are critical in preventing blockages that lead to flooding (Mugume & Butler, 2015). Furthermore, Falconer et al. (2009) underscores the importance of advanced warning systems, accurate mapping, and integrated flood management approaches to address the growing challenges of pluvial flooding. These strategies are vital for mitigating the impacts of intense rainfall events on urban areas and enhancing the overall resilience of communities.

Historically, urban drainage design has focused on a probabilistic-based system design after certain recurrence intervals. However, to create resilience, a risk-based

paradigm shift is needed that includes probabilistic assessments of both the likelihood and risk of diverse flood scenarios. (Haghighatafshar et al., 2020; Schmitt et al., 2020)

In Uganda, while only 26% of the population lives in urban areas, the country is experiencing a fast rate of urbanization (Pérez-Molina et al., 2017). Moreover, the capital city, Kampala, frequently experiences severe pluvial flooding, not only due to extreme rainfall but also because of increasing urbanization resulting in more impervious surfaces, inadequate urban drainage systems (UDSs), and lack of sufficient cleaning and maintenance of these systems (Mugume & Butler, 2015). These floods occur across the city, primarily in low-laying valleys that are characteristic for Kampala. Flooding impact all socio-economic groups, however, people experiencing poverty that live in low-lying areas are most vulnerable (Sliuzas et al., 2013).

1.2 Problem description

In Kampala, Uganda, heavy rains often lead to significant flooding due to sediment and garbage accumulating in the drainage channels (UNDP, 2023). One significant study conducted by the United Nations Development Programme (UNDP) highlights the impact of poor waste management and inadequate drainage systems in the city. The research shows that heavy rains lead to the accumulation of sediment and garbage in drainage channels, which results in blockages and subsequent flooding in various parts of Kampala (UNDP, 2023). Today, the primary channels are cleaned from sediment and solid waste twice a year in by the Kampala Capital City Authority (KCCA) (H, Wasswa, personal communication, March 15, 2024). Human factors, such as poor urban planning, inadequate infrastructure and improper waste management are common issues that regions with flooding have experienced, which can worsen drainage systems and contribute to increased flood risk (Echendu, 2023).

When flooding occurs today particularly in urban areas in developing countries, this results in several negative outcomes – both for the environment but also for the inhabitants (Chereni et al., 2020; NatuReS., n.d; Oteng-Ababio et al., 2024). Health issues arise from water contamination and the spread of diseases like cholera and malaria (Chereni et al., 2020). Property damage is extensive, affecting homes, businesses, and infrastructure, leading to economic disruptions and loss of livelihoods (Oteng-Ababio et al., 2024). Educational activities are also impacted as schools close, and materials are damaged. Moreover, repeated flooding increases the vulnerability of impoverished communities, trapping them in a cycle of poverty

(Echendu, 2023). These factors underscore the urgent need for effective flood management and resilient infrastructure to mitigate these adverse effects.

Climate change intensifies sediment-related flooding problems by increasing the frequency and intensity of rainfall events. This can lead to more severe erosion and greater sediment loads in drainage systems, further highlighting the need for adaptive management strategies (IPCC, 2018).

By developing a predictive model, I hope to aid future flood management efforts. This model has significant potential for further development, allowing other researchers to build upon it and enhance flood prevention strategies.

1.3 Main objective and research questions

The main objective of this study is to investigate how both current and increased sediment and solid waste deposits in the urban drainage system affect flooding within the upstream Lubigi catchment area. Additionally, the study aims to identify critical points vulnerable to flooding, considering current sediment and solid waste deposits.

To meet these objectives, the following research questions are raised:

- What are the most critical points vulnerable to flooding in the catchment area, considering the existing urban drainage system with current sediment- and solid waste deposition and extreme rainfall?

- What is the volume of flooding within the catchment area during different scenarios, including various sediment and solid waste deposits in the urban drainage system and during extreme rainfall events?

2. Theory

The following chapter describes key concepts essential to understanding the master thesis project, starting with explaining urban drainage and its central concepts, followed by describing sediment and solid waste. Lastly, rainfall is described.

2.1 Urban drainage

Urban drainage systems (UDSs) are needed in developed urban areas due to the disturbance of anthropogenic activities to the natural hydrological cycle. There are two main disturbances in the hydrological cycle. The first involves the extraction of water to secure a supply for human consumption and use. The second is the shift from permeable to impermeable land surface that redirect rainwater away from the natural system of drainage. These two disturbances results in two types of water: wastewater and stormwater. (Butler & Davies, 2011)

Urban drainage systems can generally be classified into conventional and sustainable urban drainage systems (SUDS) (Hellmers et al., 2018). Conventional systems typically include pipes, manholes and channels designed to quickly remove water from upstream to downstream areas to reduce the risk of flooding (Jemberie, Melesse & Abate, 2023). SUDS, on the other hand, integrate natural processes to manage water close to its source, using Blue-Green Infrastructure (BGI), such as green roofs, rain gardens, and permeable pavements to enhance infiltration and reduce runoff (Mugume et al., 2024).

Pipes and channels are the most common components of traditional UDSs, designed to transport stormwater and wastewater efficiently. However, their capacity can be overwhelmed during heavy rainfall events, leading to urban flooding (Yazdanfar & Sharma, 2015). BGI includes elements such as wetlands, swales, and detention basins that work with natural hydrological processes to manage water sustainably. BGI not only mitigates flooding but also provides co-benefits like improved water quality, increased biodiversity, and urban aesthetics (Liao et al., 2017).

In Kampala, Uganda, the urban drainage system faces significant challenges (Mugume et al., 2024). The city's drainage infrastructure, consisting of both conventional pipes and channels, often becomes clogged with sediment and solid waste, further reducing its capacity to handle heavy rainfall (Mugume et al., 2024). Potential to enhance the resilience of Kampala’s drainage system include integrating BGI to complement existing infrastructure (Mugume et al., 2024; Xueqin et al., 2022). This approach not only addresses the immediate need for effective

stormwater management but also promotes sustainability and resilience against future climate-related challenges (Kozak et al., 2020).

2.1.1 Stormwater

Stormwater is commonly understood as the water that results from rain (Bohman, Glaas & Karlson, 2020). In urban areas, stormwater runoff can pick up pollutants from various surfaces like roads, rooftops, and parking lots, including heavy metals (Yang & Li, 2013), leading to water quality issues in receiving water bodies (Bohman, Glaas & Karlson, 2020). Effective stormwater management is crucial to mitigate the negative impacts of this runoff, which include flooding, water pollution, and erosion (EPA, 2024). Stormwater management is a critical aspect of urban planning that is facing challenges due to climate change impacts, aging infrastructure, and the increasing imperviousness in cities (Barbosa, Fernandes & David, 2012).

Urban cities are facing increasing challenges in managing stormwater due to frequent heavy rainfalls intensified by climate change. Traditional urban drainage systems struggle to handle large volumes of surface runoff, prompting the need for new strategies (Chang et al., 2018). Sustainable stormwater strategies focus on reducing impervious surfaces, managing runoff and pollution at its source, and delivering various benefits such as flood mitigation, pollutant reduction, groundwater replenishment, recreational spaces, increased biodiversity, and enhanced urban aesthetics (Bohman, Glaas & Karlson, 2020). One key aspect of stormwater management focuses on reducing runoff volumes and improving water quality. This involves capturing and utilizing stormwater to reduce peak flow rates and volumes, thereby mitigating flood risks (Yang & Li, 2013).

2.1.2 Flood control

Flood control involves methods and measures made to mitigate the impact of flood disasters. Flood control can be divided into two types: structural and non-structural measures. Structural measures are aimed to manage and mitigate the impact of flooding by directly controlling the flow and storage of water. Structural measures can include improving channels to enhance their capacity to carry water more efficiently. This can be done by modifying the channels or building flood walls. The purpose is to increase the flow of water through vulnerable areas to less vulnerable areas. On the opposite side, catchments treatment is example of measures to slow down the flow and retain water before releasing it into streams and rivers. (Ghosh, 2014)

Non-structural measures, on the other hand, are strategies aimed to continue normal public and industrial activities during floods, instead of changing the physical environment (Poussin et al., 2012). Example of these measures are flood risk mapping and land use strategies to prevent development in flood-prone areas. Other examples are flood forecasting and warning systems (Ghosh, 2014).

There are also measures that combine both structural and non-structural with the purpose of mitigating pluvial flooding, reducing runoff, and lowering peak flows (Costa et al., 2021). However, the terminology differs depending on the region. Sustainable Urban Drainage Systems (SUDS), Low Impact Development (LID), Best Management Practices (BMP), Water Sensitive Urban Design (WSUD) are some examples (Fletcher et al., 2015). Blue-Green Infrastructure (BGI) is a relatively new term that uses similar practices as the above terms but includes a wider perspective of multiple ecosystem services including biodiversity, water quality, reducing thermal effects and social aspects (Liao et al., 2017).

BGI has shown to reduce pluvial flooding in Malmö, Sweden. In 2014, Malmö was exposed to a cloudburst corresponding to a return period of 50- 200 years. The neighbourhood Augustenborg includes different BGI measures like ponds, swales and green areas. After the cloudburst, Augustenborg shown more resilience than other neighbourhoods in Malmö that have conventional sewer systems. (Sörensen & Emilsson, 2018)

In a case study in Kampala, Uganda by Mugume et al. (2017) multifunctional rainwater harvesting (RWH) methods has shown to be effective against flooding and simultaneously provide households with water supply.

2.1.3 Backwater effect

Regarding an open channel, subcritical flows means that the upstream flow is controlled by the downstream conditions. This can be due to an obstacle, a change in the cross-section or a structure. For example, a downstream control structure like bridge piers or a weir can induce a backwater effect, causing water levels to rise upstream. (Chanson, 2004)

Wang et al. (2019), studied how river flow junctions affect the stage-discharge relationship in open channel systems. Their results show that backwater effects and flow separation at flow junctions influence the flow structure and patterns in the channel, that can lead to flooding disasters within the river flow junction.

2.1.4 Wastewater

Wastewater can be seen as the primary liquid waste of the community. The origin is from WCs, industry and other water uses. If it is not treated properly, or if flooding overwhelms the UDSs, it can cause pollution and health risks. Wastewater contains dissolved material and fine- and larger solids. (Butler & Davies, 2011)

In developing countries, a significant portion of the wastewater released to freshwater bodies does not undergo any form of treatment. In some urban areas, different wastewater treatment facilities (WWTF) exist. However, many of these facilities generate mistreated discharge, released into streams, ponds, and wetlands (Edokpayi et al., 2017).

2.1.5 Sediment and solid waste

Sediment and is commonly found in urban drainage systems. Its movement through a catchment involves multiple complex stages. For example, sediment deposited on roads is first released from the surface and then carried sideways by overland flow to the channel, where it travels along the road edge under open channel flow. (Butler & Davies, 2011)

When entered in open channels, the sediment is transported mainly by suspended- and bed load transport. Suspended load transport includes material that is mainly transported downstream in suspension, distant from the bed, but still interacts with the bed due to sedimentation and turbulent mixing. Conversely, bed load remains near the bed, moving primarily through rolling or short jumps. (Lyn, Chen & Liew, 2003)

Urban development activities, including construction and deforestation, significantly contribute to sediment production. Erosion from construction sites can introduce large amounts of sediment into stormwater systems. Strategies to control erosion, such as silt fences and sediment basins, are crucial in mitigating this issue (Prosser et al., 2001). Moreover, sediment deposition is a critical factor influencing water flow dynamics and impact pressure on bridge decks during flooding (Niu et al., 2023). Sediment deposition refers to the accumulation of sediments, such as sand, silt, and debris, on the riverbed (Tang et al., 2020).

Effective sediment management strategies are essential for maintaining the capacity and functionality of urban drainage systems. These can include regular maintenance and cleaning of drainage systems, the installation of sediment traps, and the implementation of green infrastructure solutions such as vegetative swales and retention basins (Dietz, 2007).

Sediment deposition is influenced by natural processes such as flood events, where sediments are transported from the catchment area to the floodplain downstream of hydraulic structures (Mahmood et al., 2022).

In developing countries, solid waste is commonly found in the urban drainage system, causing blockage which result in flooding (Stevaux et al., 2009; Mokuolu et al., 2022). Urban managers have focused on improving physical infrastructure, such as clearing urban drainage systems; however, with limited success (Zambrano et al., 2018).

2.2 Rainfall

Most of the water that is referred to as stormwater originates from rainfall. Therefore, when analysing urban drainage, it is crucial to be able to represent and predict rain. To measure rainfall, rain gauges is the most common method. Rainfall measured at a single rain gauge is typically expressed as data of depth in mm or intensity in mm/h. However, this data is only a representation of a certain position in the catchment. The value of the data significantly increases when it can be statistically associated with duration and frequency. The duration is defined as the time in minutes over which the rainfall falls. Nevertheless, a rainfall event can be divided into several durations to be analysed separately. The frequency or probability is often denoted as a return period or recurrence interval. The return period is defined as the interval, T years, within which an annual maximum rainfall is expected to occur once, on average, with magnitude equal to or greater than a specified amount. For example, a rainfall with a return period of 5 years is expected to occur on average 20 times in 100 years, which corresponds to a probability that is equalled or greater of 0.2. It is important to note that it is assumed that the maximum event in one year is statistically independent of the maximum event in any other year. (Butler & Davies, 2011)

However, the IPCC (2023) states that a temperature increase of 4°C relative to pre-industrial levels will result in a non-linear increase of the frequency of heavy rainfalls. It is likely that events with a return period of 10 years and 50 years will occur with double and triple frequency, respectively. Additionally, the intensity of heavy rainfall on a regional extent will fluctuate, due to amount of regional warming, variations in atmospheric circulation and storm dynamics. In Sweden, a climate factor is applied to the rain intensity to account for this increase in intensity due to climate change (SWWA, 2016).

2.2.1 IDF curves

One of the most widespread tools when designing, planning, and managing water resource projects is the Intensity-Duration-Frequency (IDF) relationship (Koutsoyiannis et al., 1998). IDF curves effectively illustrate the expected rainfall within a specific region, demonstrating the average rainfall intensity for each return period and across all durations of rainfall events (Basumatary & Sil, 2017). In Figure 1, for a given return period, a high intensity results in a low duration, and vice versa. It also shows that the intensity increases with the return period.

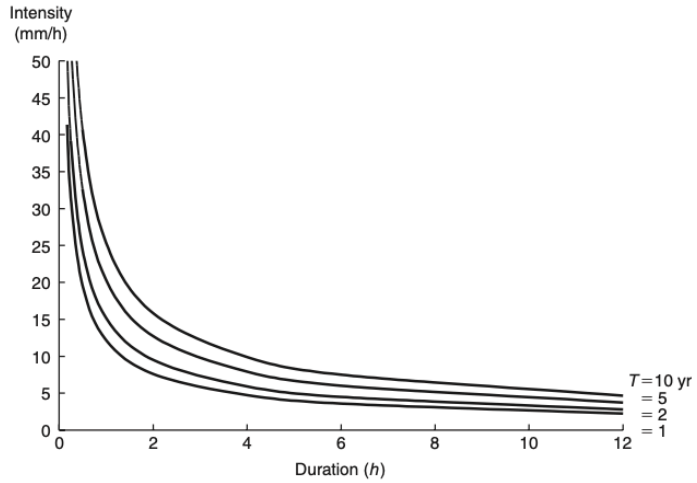

Figure 1 Typical IDF-curves (Butler & Davies, 2011)

There are discussions globally that IDF curves need to be updated to cover for climate change. However, it is a difficult task. Kourtis & Tsihrintzis (2022) reviewed more than 100 articles published between 2001 and 2021 and concluded that there is a need for long-term and high-resolution rainfall-data from multiple gauging stations to capture the spatial patterns of rainfall. In developing countries especially, this is a difficult task which make future changes due to climate change hard to estimate.

2.2.2 Annual Maximum Method

To derive IDF curves, the Annual Maximum Method (AMS) can be used. The method involves collecting the highest recorded rainfall depths from a continuous record. The annual maximum values are then ranked from 1 to number of years or record. The desirable return period can then be estimated using Weibull's plotting position formula (Equation 1). (Butler & Davies, 2011)

$$T = \frac{n+1}{m}$$

Equation 1 Weibull's plotting position formula where T is the return period, n is number of records and m the event rank number (1,2,…n) (Butler & Davies, 2011).

2.2.3 Design storms

As stated, the IDF curves provide information about the rainfall intensity, duration, and frequency. However, how the rainfall intensity varies over the duration of a storm is not presented. Therefore, design storms are used by extracting values from IDF curves. One of the most representative in hydrology is the Alternating Block Method (Balbastre-Soldevila, García-Bartual & Andrés-Doménech, 2019).

The procedure uses intensities from the IDF curve for a given duration. The duration is thereafter divided into smaller time intervals and ranked from high to low. After this the highest intensity is placed in the centre of the storm duration and the rest of the intensities is altered before and after according to rank. This finally results in a more real-life representation of a storm than only using the IDF curve. (Chow et al., 1988)

The final step of creating design storms is to account for that the data collected from a rain gauge is a point data. To adjust this, areal reduction factors (ARF) have been developed (Butler & Davies, 2011). The ARF value is multiplied to the derived rainfall intensities.

3. Materials and Methods

The following chapter includes the material and methods used to conduct this study. The chapter will begin with a case study conducted in the upstream Lubigi catchment area. Thereby, a description of the methods and materials will follow.

3.1 Upstream Lubigi catchment area

A case study was conducted in the upstream part of the Lubigi catchment (Figure 2). The catchment area is 33 km^2, in comparison to 64 km^2 for the whole Lubigi catchment. The upstream part consists mainly of urbanized areas, 1 primary channel and 8 secondary channels. In the downstream part of the main channel, water flows via Lubigi wetland which is one of the largest wetlands in Kampala (KCCA, 2016). Before the wetland, water flows close to the Lubigi sewage treatment plant.

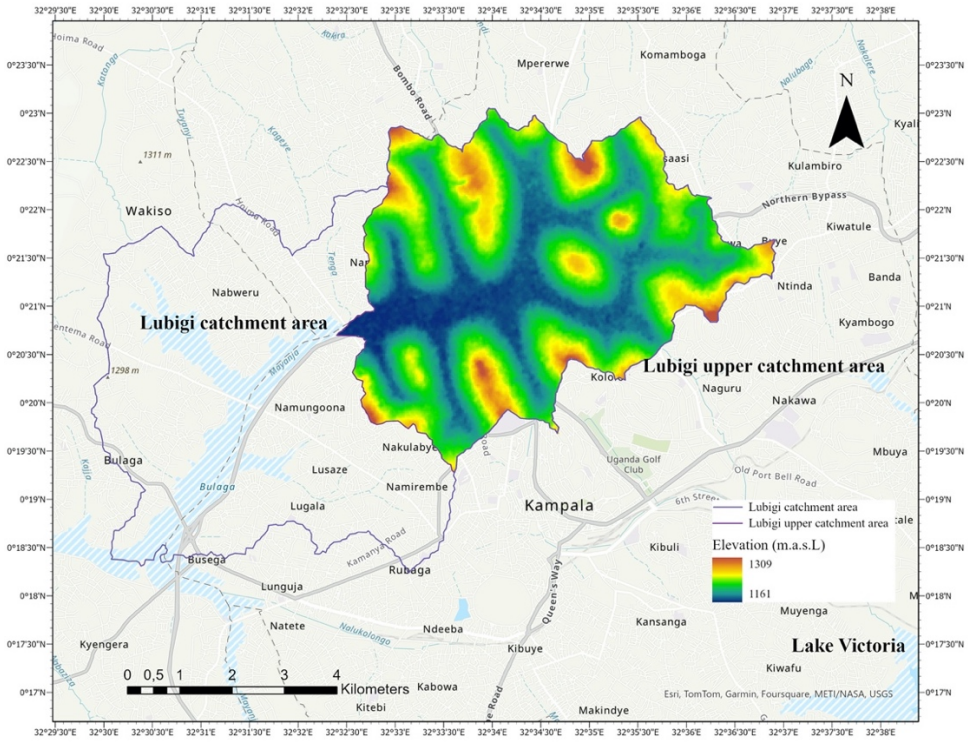

Figure 2 Lubigi catchment area with the upstream part of Lubigi catchment included with elevations.

Lubigi catchment is frequently exposed to pluvial flooding. In 2016, Kampala Capital City Authority (KCCA) conducted an interview study where they stated that 69% of the households interviewed had experienced flooding within Lubigi catchment, which is the highest percentage of all the catchment areas in Kampala (KCCA, 2016). One of the driving forces of flooding is the blockage of silt and solid waste in the channel and culvert crossings (Figure 3). De-silting is executed on an ad-hoc basis using excavators. However, in some cases the width of Lubigi channel is wider than the boom of the excavator. The result of this is that an island of silt is left in the middle of the channel, which works as a driver for flooding (KCCA, 2016).

Figure 3 Silt- and solid waste in Lubigi primary channel

The urban drainage system can be divided into the "minor system" and the "major system". Kampala Capital City Authority (KCCA) define the minor system as small drains between buildings and the roadside drainage. The purpose of the minor system is to convey stormwater to the major system in such a way that inconvenience to pedestrians and vehicular traffic is minimized. The major system consist of large open channels and culverts used to transport water to the recipient.

The average annual rainfall depth for Kampala is 1292 mm (Mugume, 2015). Kampala has two major rain seasons occurring from March to May and from September to November (Nimusiima et al., 2021). April is the wettest month, with approximately 180 mm of average monthly rainfall, while July is the driest month, receiving around 60 mm of average monthly rainfall (Mugume, 2015).

3.2 Methods

This study investigated the hydraulic impacts of sediment- and solid waste deposition during varied hydraulic conditions. In combination with sediment and solid waste deposition, different rainfall events were modelled based on recent observed rainfall and observed historical rainfall (IDF curves) with a fixed duration of 30 hours and varied return periods of 2, 10, 50, and 100 years. The time of concentration for the upper catchment area were assumed to be less than 30 hours. This was based on the time of concentration for the Nalukolongo and Kinawataka catchments (Mugume et al., 2024) in Kampala which has similar characteristics as the upper Lubigi catchment area. Therefore, a fixed duration of 30 hours was used for all design storms.

A 1D hydraulic model was built in PCSWMM, based on drawings from KCCA, Digital Elevation Maps (DEMs) and field visits. To make proper calibration and validation of the model, a rain gauge and a water level meter were installed, and several field observations were made to verify the technical drawings of the urban drainage system.

This study used PCSWMM developed by Computational Hydraulics Inc (CHI) for creating the 1D-model. PCSWMM is a widely used modelling program for water resource studies all over the world (Chitwatkulsiri et al., 2022; Mugume et al., 2024; Ortega Sandoval et al., 2023). PCSWMM uses the EPA SWMM5.2 dynamic rainfall-runoff simulation engine (Rossman & Simon, 2022) along with support tools like GIS technology. SWMM5.2 uses a physically based, discrete-time simulation model where the surface runoff outflow and the open channel flow is calculated using Manning's equation (Equation 2):

$$Q = \frac{1}{n} AR^{2/3} S^{1/2}$$

Equation 2 Manning's equation where Q is the flow, n is Manning's roughness coefficient, A the cross-sectional area, R the hydraulic radius and S the slope of the energy grade line (friction slope).

In addition, the flow routing in closed and open conduits follows the Saint-Venant's equations for continuity (Equation 3) and momentum (Equation 4):

$$B\frac{\partial y}{\partial t}+\frac{\partial Q}{\partial x}=0$$

Equation 3 Saint-Venant's continuity equation where B is the width, y the depth, Q the flow and x the distance (Butler & Davies, 2011).

$$\frac{\partial Q}{\partial t}+\frac{\partial}{\partial x}\left(\frac{Q^2}{A}\right)+gA\frac{\partial y}{\partial x}-gA\left(S_0-S_f\right)=0$$

Equation 4 Saint-Venant's momentum equation where Q is the flow, t the time, x the distance, A the cross-sectional area, g the acceleration due to gravity, y the depth, S_0 the bed slope and S_f the friction slope (Butler & Davies, 2011).

In PCSWMM, the user can choose between three methods of flow routing: Steady flow routing, Kinematic wave routing and Dynamic wave routing. Steady flow routing represents the simplest method by assuming that within each computational time step, the flow is uniform and steady. Kinematic wave routing is more extensive. This method solves the continuity equation (Equation 3) and assumes a simplified solution for the momentum equation (Equation 4), where the bed slope (S_0) and the friction slope (S_f), is assumed to be equal. Using this form of routing, the model can not account for backwater effects, flow reversal, entrance/exit losses or pressurized flow. Dynamic wave routing is the most comprehensive routing method, involving calculations of the full Saint-Venant flow equations (Equation 3) and (Equation 4). This approach can represent pressurised flow, with flooding occurring when the water depth at a node surpasses the maximum available depth. The flooded volume is either lost from the system or ponded on-top of a node and re-entered to the system when capacity is available. Dynamic wave routing can, in contrast to Steady state- and Kinematic wave routing account for backwater effects, flow reversal and entrance/exit losses. (Rossman & Simon, 2022)

In this study, Dynamic wave routing was used without allowing ponding, meaning that when a node floods, the flooded volume is lost from the system.

3.3 Experiment design and scenario description

The modelling of current sediment and solid waste deposition has been conducted by adjusting Manning's roughness coefficient for conduits. More detailed description is described in chapter 3.6.3 Calibration and chapter 3.6.4 Validation. The increased sediment and solid waste deposition has been modelled by reducing the cross-sectional areas of culvert crossings (Aksoy et al., 2017), at locations where sediment and solid waste today is accumulated. These locations where chosen based on observations during field visits.

The modelling experiment were performed by running the model with 4 extreme rainfalls of duration of 30 hours and return periods of 2, 10, 50 and 100 years. The experiment was conducted by these 3 steps:

Scenario 1: Current sediment- and solid waste deposition

Existing UDSs with current condition of sediment and solid waste deposition. This condition is represented by adjusting Manning's roughness coefficients for conduits, which has been calibrated and validated.

Scenario 2: Moderate accumulation

Culvert cross-sectional area reduced by 50% at three locations (Figure 4), reflecting significant blockages but not complete. This simulation helped understand the potential increase in flood risk and the system performance degradation under moderately neglected maintenance conditions.

Scenario 3: Severe accumulation

Culvert cross-sectional area reduced by 80% at three locations (Figure 4), representing near-complete blockage. This severe scenario tested the system's resilience under extreme sediment and solid waste deposition conditions.

Figure 4 show the three locations used for modelling the increased sediment and solid waste deposition. These locations were chosen because of their critical location in the urban drainage system and because sediment and solid waste currently is being accumulated here, based on field visits.

Figure 4 Culvert crossings with sediment and solid waste blockage used for Scenario 2 and Scenario 3.

3.4 Tipping Bucket Rain Gauge

A HOBO Data logging Rain Gauge RG3-M was installed on Wednesday, 28 February 2024, to obtain high-resolution rainfall data. The tipping bucket rain gauge was installed within of Lubigi sewage treatment plant (0.3474310, 32.5487220) to minimize unwanted interference from individuals with the device. To avoid splashing and puddles, the rain gauge was mounted 50 cm above ground on top of a wooden construction. The rain gauge was mounted in a level position using a bubble level inside of the rain gauge (Figure 5).


Figure 5 Tipping bucket rain gauge mounted 50 cm above ground.

3.4.1 Calibration of Tipping Bucket Rain Gauge

The tipping bucket rain gauge was calibrated in accordance with the HOBO Data logging Rain Gauge RG3-M manual (HOBO, n.d.). The following materials were used to calibrate the model:

- Plastic container of 1,2 litre containing a small hole (a pinhole) in the bottom.
- Two plastic measuring glasses of 1,2 and 1,2 litre.
- Two wooden sticks.
- 2 litres of water.
- RG3-M Rain Gauge.
- Tools

The field calibration took place on Wednesday, 28 February 2024, at the Lubigi sewage treatment plant in Kampala. It was a clear, sunny day, with no rain. The calibration proceeded as follows:

The wooden sticks were first placed on the rain gauge, followed by positioning the plastic container on top of them (Figure 6). The pinhole was positioned so that the water did not drip directly down the funnel orifice.

- 373 ml of water was measured with the two plastic measuring glasses and was poured into the plastic container.
- Every tip was recorded with the logger until the plastic container was empty.

The first calibration took approximately 2 hours and resulted in 105 tips. In accordance with the manual, successful field calibration should result in 98-102 tips. Due to the observed events being outside of the range, the adjusting screws were turned 1 turn counterclockwise which decreases the number of tips by approximately 4 events. The field calibration was executed a second time which took approximately 2 hours and resulted in 101 tips. The rain gauge was then determined to be successfully calibrated.

Figure 6 Calibration setup with plastic measuring glasses to the left.

3.4.2 Observed rainfall

Figure 7 show four of the largest observed rains in March and April using the tipping bucket rain gauge. All four rainfall events peak in the beginning of the rainfall, approximately within the first 30 minutes. However, there are some different characteristics. The two rains on the top, from 10 of March and 23 of April 2024 have large peaks in the beginning containing the major volume from the rainfall. And the two rainfalls in the bottom of the figure, from 21 of April and 6 of March have their rain volume more spread out during the event.

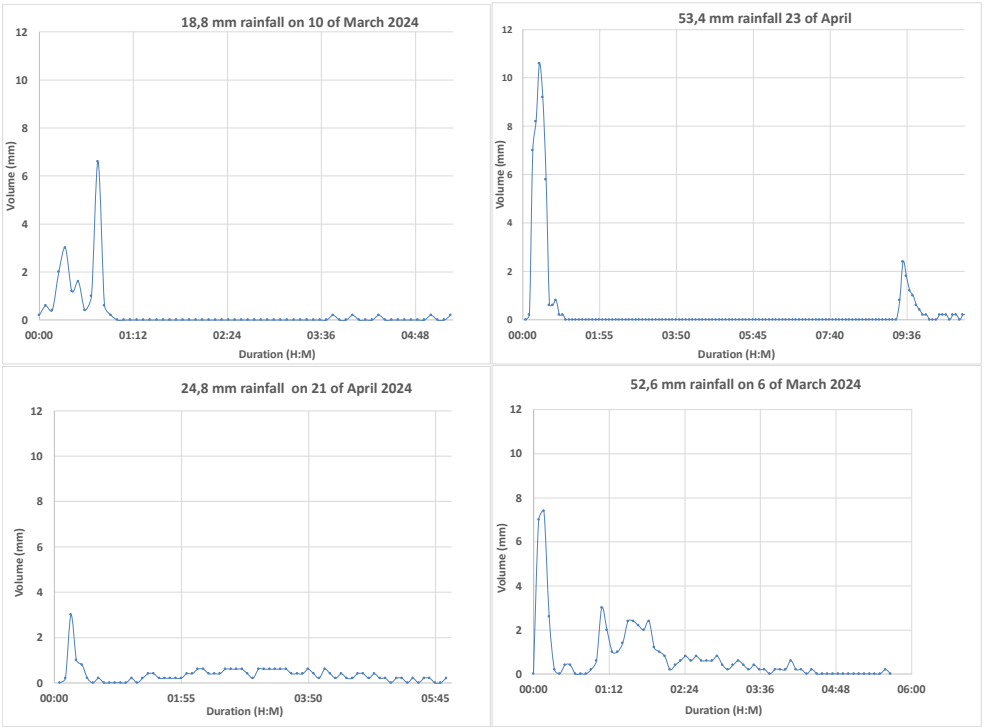

Figure 7 Rain gauge observations from March and April.

3.5 Water Level Observations

A water level meter was installed near the Hoima culvert, on Friday, 1 Mars 2024, in the Lubigi main channel. This location is later in the report referenced to as the Police station. The water level meter is located within the Lubigi wetland (0.346963, 32.540669). The meter was screwed onto a 3 m stainless-steel angle bar and pressed down 1 m down in the channel (Figure 8).

Figure 8 Water level meter located in the Lubigi main channel.

A second water level meter is located 60 m upstream of the above installed water level meter (0.347107, 32.541358) (Figure 9). The water level meter is attached to a box culvert along Hoima Road and was installed by the Uganda Ministry of Water and Environment (S. Mugume, personal communication, February 28, 2024).

Figure 9 Water level meter located on a box culvert along Hoima Road.

Measurements from both water level meters were taken twice daily: one measurement in the morning and a second measurement in the afternoon. However, if it was raining during the day, the measurement was taken after the rain to account for all the additional water resulting from the rainfall. If the rainfall had been occurring during the night, then peak indicators on culvert crossings has been noted (Figure 10).

Figure 10 Peak indicator of water level on culvert.

3.6 The Model

The model of the existing UDS that drain the upstream Lubigi catchment area were built as a 1D hydraulic model in PCSWMM. The primary and secondary channels consist mainly of open trapezoidal channels of concrete, stone pitching and earth material. The open channels connect with concrete box and pipe culverts. In 2020-2021, the main channel from Gulu Highway to Hoima Road and secondary Nakamiro channel was relined using concreate lining (KCCA, 2020). The 1D-model setup was applied using case study specific data described in Table 1.

Table 1 Information of different types of data used in the 1D model

Data set	**Data quality**	**Data period or year of publication**	**Source**	**Purpose**
Tiping bucket rain gauge	High-resolution rainfall (mm)	February -May 2024	Primary source	Extreme rainfall analysis
Staff water level gauge	Water level (m)	February – May 2024	Primary source	Model calibration
77-year daily rainfall for Makerere University rain gauge station	Daily rainfall (mm)	1943-2019	Uganda National Meteorological database (Seiths publication)	Extreme rainfall analysis
Shuttle Radar Topography Mission (SRTM) Digital Elevation Model	30 m spatial resolution	2014-09-23	United States Geological Surveys (USGS) SRTM	Digital Elevation data for identifying areas prone to flooding
Sentinel-2 satellite image	5 m spatial resolution	2023-08-22	Copernicus	Land-use and land cover analysis imperviousness (PIMP) from spectral imagery in ArcGIS
Base map World Imagery ArcGIS Pro	0.31 m (1), 0.46 m (2), 0.31 m (3) Spatial resolution	2022-10-15 (1), 2023-02-20 (2), 2023-04-16 (3)	Esri, ArcGIS Pro	Land-use and land cover analysis imperviousness (PIMP) from spectral imagery in ArcGIS
Existing and design urban drainage network data (open channels, cross culverts)	UDS parameters (bottom width, side slopes), lengths of channel sections, invert levels, slopes, cross culvert diameters	2016 and 2020	Kampala Capital City Authority (KCCA) reports and design drawings	1D urban drainage model

ArcGIS spatial analysis was conducted to delineate the catchment into sub-catchments and to calculate sub-catchment areas, percentage slopes, and widths. Additionally, surface types were calculated from spectral imagery using ArcGIS spatial analysis. The percentage imperviousness was calculated to be 74% which for simplification were applied consistent to all sub-catchments. In Figure 11 the results from spectral imagery analysis are shown.

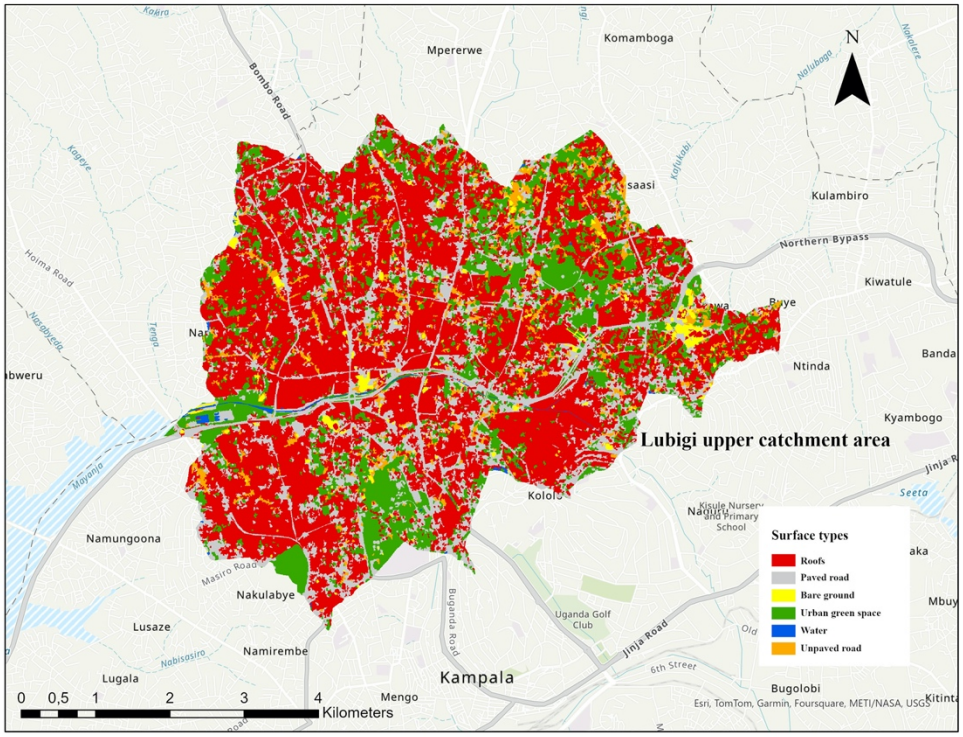

Figure 11 Surface types calculated from spectral imagery using ArcGIS spatial analysis.

Hydraulic data for the primary and secondary channels was obtained from KCCA (2016). The data used included open channel cross-section dimensions (depth, bottom widths, and sides slopes), material and length. In addition, information of culvert crossings which included cross-sectional dimensions (height, widths), type of culvert, number of barrels, material, and length. For the relined primary channel and secondary Nakamiro channel, design drawings were obtained from KCCA (2020) which included more detailed drawings than KCCA (2016) and invert levels. These invert levels were used as a base to calculate the invert levels for the rest of the catchment area using given slopes from KCCA (2016). In addition, site visits were conducted to verify the data obtained from KCCA. Data for channel width, material and culvert type were corrected for some sections after the site visits.

The modelled upper Lubigi UDS comprises of 35 sub-catchments (green), 348 conduits, 346 junctions and drains into Lubigi wetland (Figure 12). To account for water present in the downstream area that could impact the upstream catchment area, the primary channel was extended until Sentema crossing. In addition, 10 supplementary sub-catchments (blue), 9 conduits, 8 junctions and 2 outfalls were added.

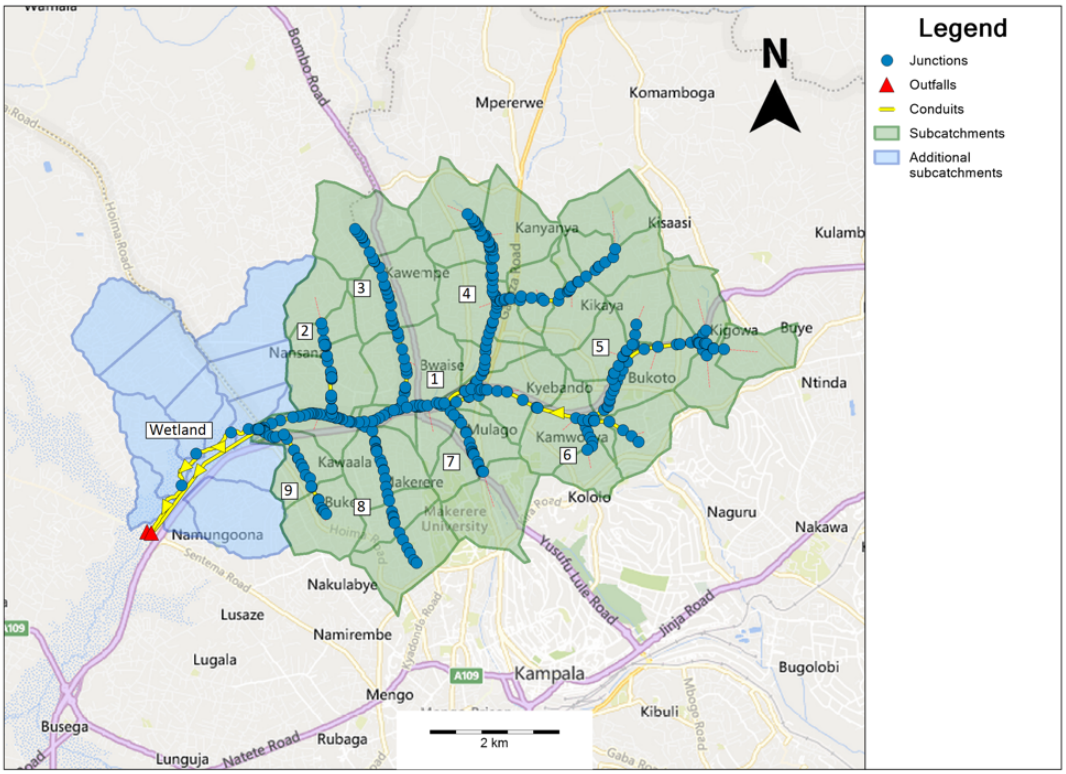

Figure 12 Overview of modelling setup in PCSWMM.

The observation point for measuring water level is located upstream of the wetland, shown in Figure 13. Cross-sectional area and the invert level 100 m downstream of Hoima crossing have been measured in the field. The same cross-section and slope have been assumed until the outfall. The wetland has been modelled as a long conduit with seepage rate and a connected outfall. The cross-sectional area and depth of the wetland were based data from (KCCA, 2016). From observations in the field, it was noted that the majority of the baseflow, that origins from shallow groundwater and wastewater (S. Mugume, personal communication, April 5, 2024), flows via the channel. However, at higher flows, water also flows into the wetland. Therefore, the wetland was assumed to connect to Hoima crossing at 0.5 m above the invert level. This results that water flow via the channel at baseflow but at higher

flows water is also converted to the wetland. A visualization of the existing wetland and channel is shown in Figure 14.

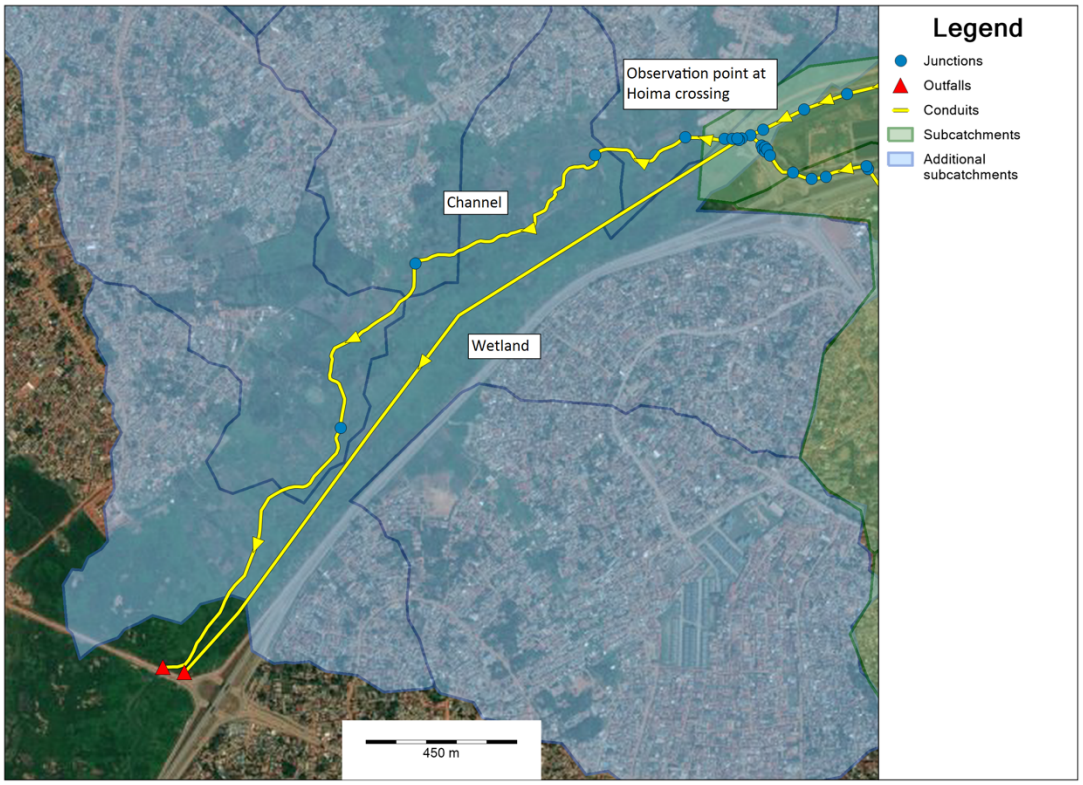

Figure 13 Modelled channel and wetland located downstream of the area of interest.

Figure 14 Existing wetland (to the left) and primary channel downstream the area of interest (to the right).

3.6.1 Extreme Rainfall Analysis

To account for extreme rainfall, Intensity-Duration-Frequency (IDF) curves for Kampala were obtained from Dr Seith Mugume and is presented in Figure 15. The IDF curves were derived using the Annual Maximum Series (AMS) method using observed 77-year daily rainfall between 1943-2019 for Kampala. To incorporate the effects of current climate change on the observed extreme rainfall, a change factor (CF) of 1.3 were applied to upscale the extreme rainfall (Mugume et al., 2015).

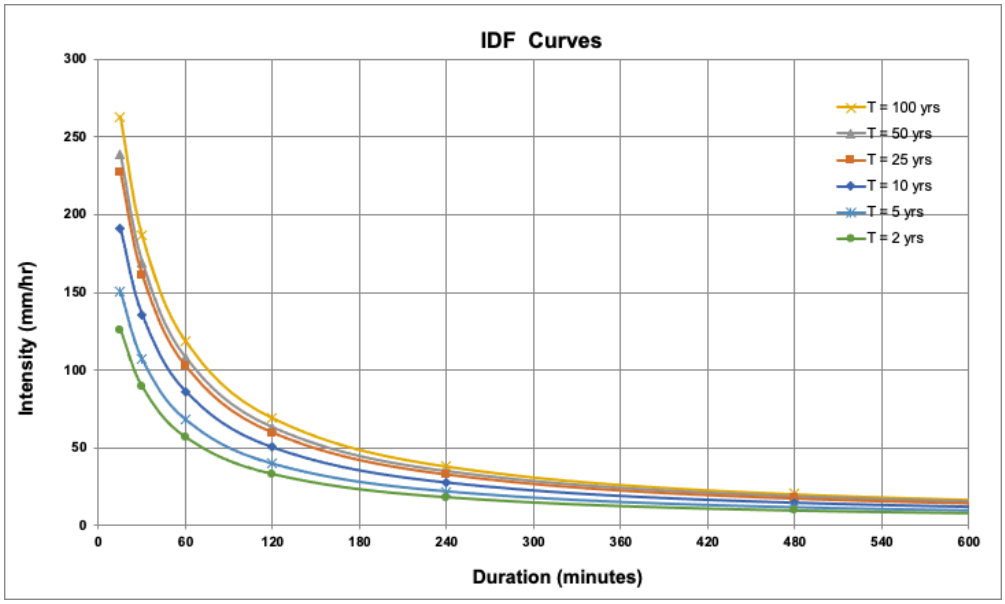

Figure 15 IDF curves for Kampala obtained from Dr Seith Mugume.

To mimic the natural occurrence of extreme rainfall, design storms were created using the alternating block method (Balbastre-Soldevila, García-Bartual & Andrés-Doménech, 2019). An Areal Reduction Factor (ARF) of 0.885 using the upstream catchment area of 33 km^2 were applied to account for the difference between a point rainfall and an areal rainfall. 4 design storms were created for return periods (T) of 2, 10, 50 and 100 years and with a duration of 30 hours. The design storms are shown in Figure 16. It should be noted that the peak of the design storms is occurring at time equal 120 minutes.

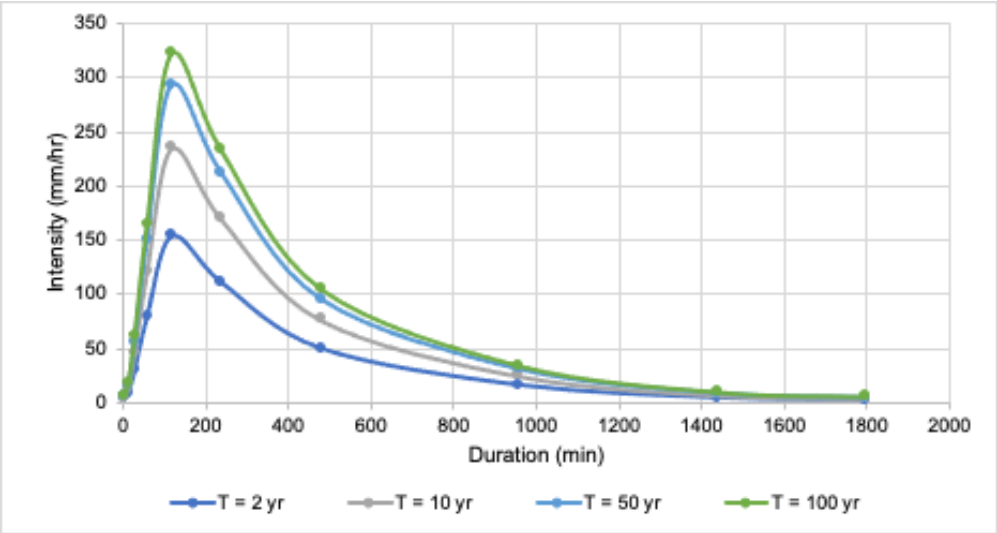

Figure 16 Design storms for Lubigi catchment area for a fixed duration of 30 hours. With the peak of the rainfall occurring at t=120 min.

3.6.2 Sensitivity analysis

A One factor at a Time (OAT) sensitivity analysis were conducted to identify the most sensitive model parameters. 15 parameters in PCSWMM were included. The parameters were changed one at a time by increasing and decreasing its value by 50% while the rest of the parameters remained unchanged. *Manning's roughness coefficient for channel flow*, *average value baseflow* and *percentage imperviousness* were determined to be the most sensitive parameters. As described above, the percentage imperviousness had been calculated by using ArcGIS spatial analysis of spectral imagery, therefore this value remained unchanged and Manning's roughness coefficient for channel flow and average value baseflow to be included in the calibration, described further down.

3.6.3 Calibration

The model was calibrated using recent observed rainfall, including a timeseries with all rains in March and measured water level at the Hoima bridge culvert. Due to uncertainties of the water level observations at the location at the Police station, because of unforeseen circumstances, these were not included in the same extent in the calibration.

The calibration included reaching peak flow, water level before and after rainfall and baseflow. The calibration focused on two rainfall events, one event on 6 of March of 53.4 mm with duration 4 and 23 minutes and one on 27 of March of 13.4 mm with

duration 5 hours and 5 minutes. The model parameters adjusted in PCSWMM to attain the measured water level were Manning's roughness coefficient for channel flow and average value baseflow.

The primary- and Nakamiro channel containing sediment and solid waste, the wetland and the channel in the wetland were assigned a Manning's roughness coefficient of 0.05. Secondary channels were assigned a Manning's roughness coefficient of 0.02 – 0.0325 depending on their specific characteristics. Culvert crossings currently containing sediment and solid waste, were assigned a Manning's roughness coefficient of 0.1. The primary channel was assigned an average value baseflow of 4 dm^3/s and secondary channels 1 dm^3/s.

3.6.4 Validation

The model was validated using a timeseries of rain events and water level observations ranging from 5 April to 23 April. A total of 40 water level observations, covering 11 rainfall events were included. To evaluate the validation the Nash-Sutcliffe Efficiency (NSE) and the Root Mean Square Error (RMSE) were calculated.

The Nash and Sutcliffe coefficient is a goodness-of-fit indicator which is calculated by subtracting the ratio of the mean square error between the observed and modelled values (Equation 5):

$$NSE = 1 - \frac{\sum_{i=1}^{N}(O_i - P_i)^2}{\sum_{i=1}^{N}(O_i - \bar{O})^2}$$

Equation 5 The Nash and Sutcliffe coefficient where O_i represent the observed values, P_i the modelled value and $\bar{O}$ the mean of the observed values.

A NSE of =1 indicates a perfect fit while a NSE =< 1 indicates that the mean observed values servers as a more accurate indicator than the model. (Ritter & Muñoz-Carpena, 2013)

The Root Mean Square Errror (RMSE) is indicator of the prediction error in a model (Equation 6). A RMSE = 0 indicates an ideal fit.

$$RMSE = \sqrt{\frac{\sum_{I=1}^{N}(O_i - P_i)^2}{N}}$$

Equation 6 The Root Mean Square Error (RMSE) where O_i represent the observed values, P_i the modelled value. A RMSE = 0 indicates an ideal fit. (Ritter & Muñoz-Carpena, 2013)

4. Results

The following chapter describes the results from the master thesis project. Starting with the model performance, followed by answering the first research question by identifying critical points for the existing UDS. Lastly, the second research question is answered by presenting a scenario analysis.

4.1 Model performance

The validation was executed for 40 water level observations during April. The Nash-Sutcliffe Efficiency (NSE) resulted in 0.81 which was considered acceptable (NSE > 0 is considered better than using the mean value of the observation series). The Root Mean Square Error (RMSE) was calculated to be 0.18 m, compared to the standard deviation which was 0.41.

In Figure 17 the modelled water levels are plotted against the observed water level to visualize the calibration and validation results. The reference line is used to see the model accuracy. A value above the line means that the model predicted above the observed value, and vice versa. A value that is present on the reference line means a perfect fit. Note that the figure also includes peak indicators of water level, see details in chapter 3.3.

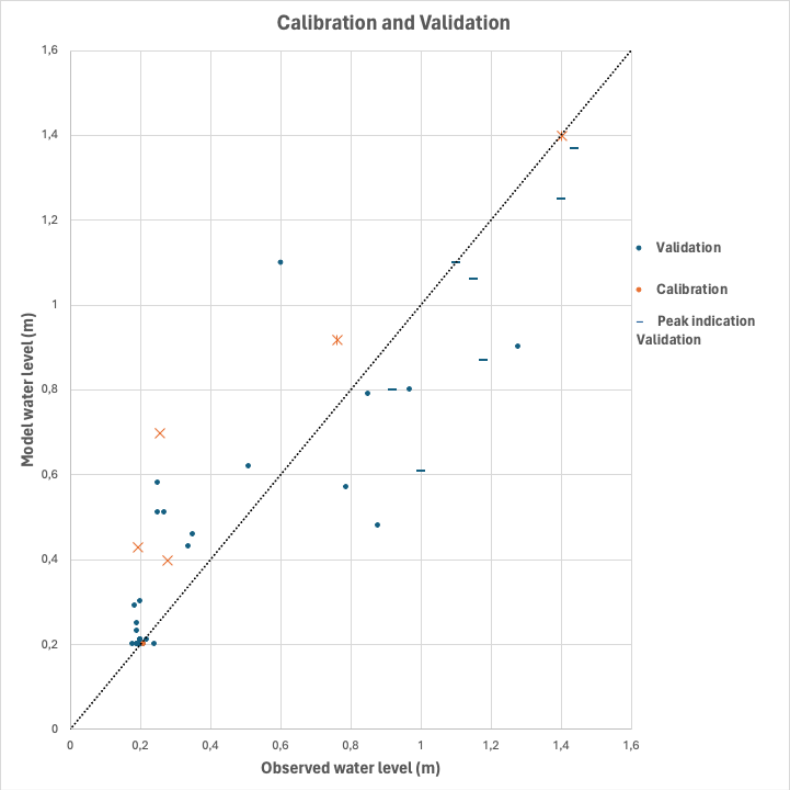

Figure 17 Calibration and validation results.

As described in the Method section, the wetland has been modelled as a large open conduit with seepage rate and an offset of 0.5 m up from the invert level. This approach mimics the natural process were, at low flow, water flow via the open channel in the wetland. However, during larger flows, water is also diverted into the wetland itself.

Figure 18 illustrates the open channel in the wetland before (1) and after (2) receiving inflow from a sub-catchment. However, in reality, water flows from the sub-catchment via secondary channels to the wetland channel, and not directly to the wetland channel as constructed in the model (Figure 18).

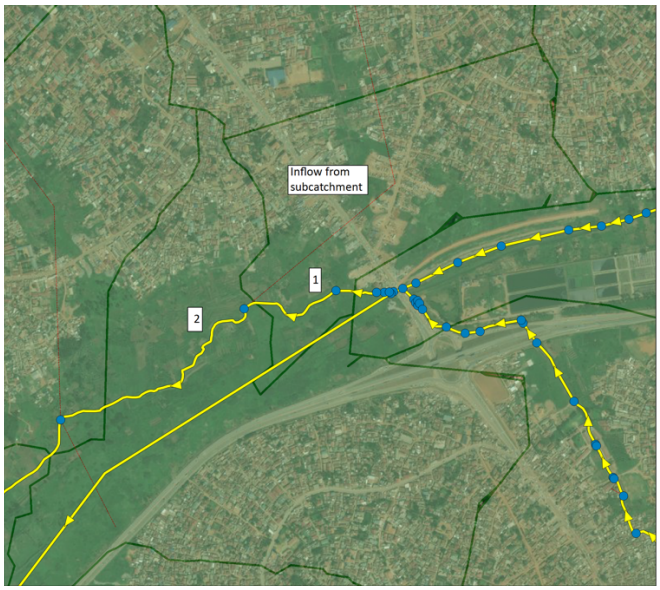

Figure 18 Visualisation of open channel present in wetland before (1) and after (2) inflow from a sub catchment.

In Figure 19, the flow in the open channel is shown before (to the left) and after (to the right) receiving inflow from the sub-catchment, simulated with the rain event T10. An oscillating flow, varying from negative to positive flow is predicted by the model before the channel. However, a non-oscillating flow after the contribution of flow from the sub catchment.

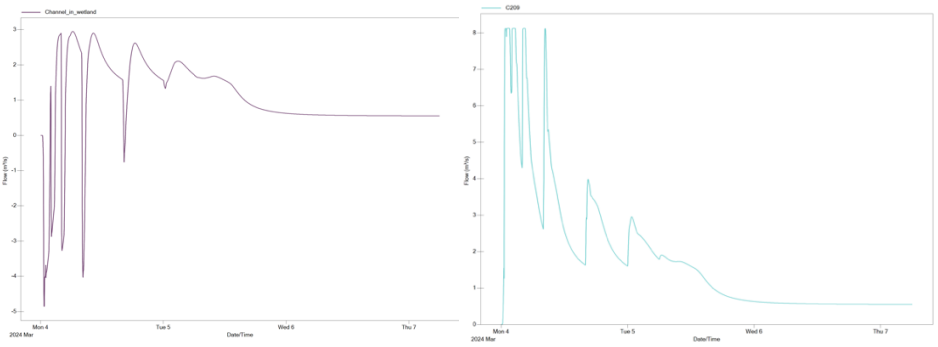

Figure 19 Channel flow in wetland before (to the left) and after (to the right) receiving inflow from the sub catchment, simulated with T10.

4.2 Critical points vulnerable to flooding

By running the model with a time series of recent observed rainfalls and current sediment and solid waste deposition, three critical points vulnerable to flooding were identified: Bwaise, Alice Kaggwa Road and Kamwokya Kisalosalo Road (Figure 20).

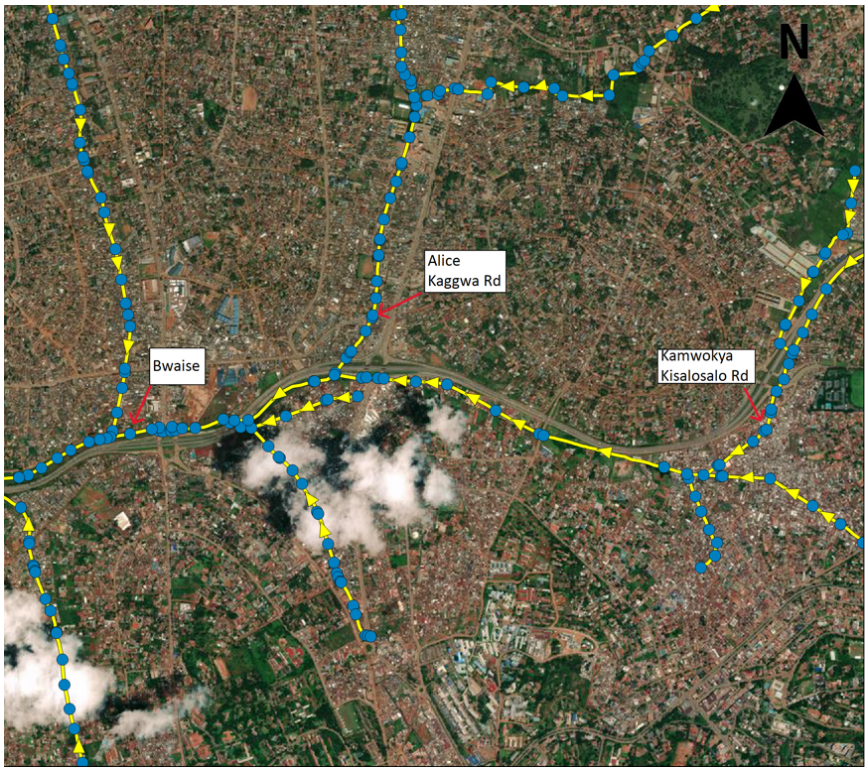

Figure 20 Three critical locations vulnerable to flooding.

Table 2 shows the flooding loss at these three locations. In the model, flooding loss refers to water that has overflowed the drainage system and is no longer part of the drainage network. This could be described as the flooded water is spread out on the surface, effectively being “lost” from the drainage system and not returning to the source.

For the rain event on March 6, 2024, flooding at these three nodes accounted for 57% of the total flooding in the catchment. For the synthetic T10 and T100 rain events, flooding was approximately 20% compared to the entire area. By comparing these rainfalls, the observed rainfall on March 6 was 52,6 mm over a duration of 5,5 hours, while the synthetic T10 and T100 rain events included depth of 113,7 mm

and 156 mm respectively, both over a duration of 30 hours. This indicates that as rainfall events increase in both volume and duration, the flooding becomes more dispersed throughout the catchment.

Table 2 Flooding loss and the sum of flooding loss compared to the entire catchment for three indentified critical points.

Rainfall	Bwaise Flooding loss	Alice Kaggwa Road Flooding loss	Kamwokya Kisalosalo Road Flooding loss	The sum of flooding loss compared to the entire catchment
03-06-24 (52.6 mm)	149 000 m^3	64 000 m^3	78 000 m^3	57%
T10 (113.7 mm)	209 000 m^3	94 000 m^3	140 000 m^3	19%
T100 (156.4 mm)	252 000 m^3	115 000 m^3	176 000 m^3	20%

4.2.1 Bwaise

Starting with the location at Bwaise. This point is located downstream of the catchment area, receiving water upstream from 4 secondary channels. In Figure 21 the Bwaise flooded node is shown. The figure also highlights the Nakamiro crossing, where (1) is located upstream of the crossing on Lubigi channel, (2) is located upstream of the crossing on Nakamiro channel and (3) downstream the crossing.

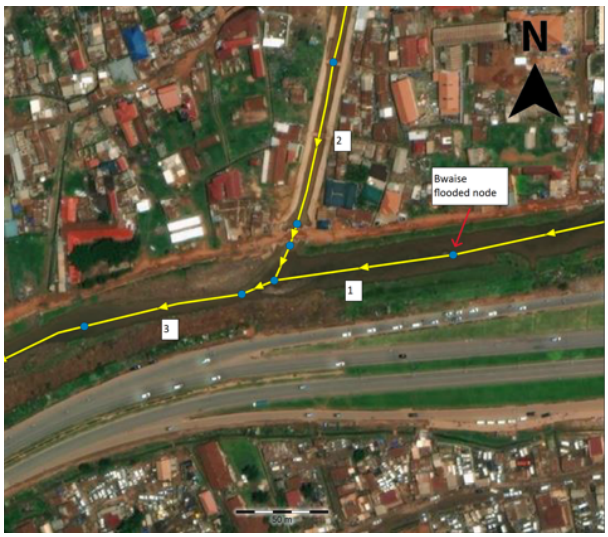

Figure 21 Nakamiro crossing where (1) is located upstream of the crossing on Lubigi channel, (2) is located upstream of the crossing on Nakamiro channel and (3) downstream the crossing.

Figure 22 and Figure 23 shows flow, depth, and velocity hydrographs for location (1), upstream of the crossing on the Lubigi channel, and location (2), upstream the crossing on the Nakamiro channel.

The maximum flow rates are 20 m³/s for the Lubigi channel and 16 m³/s for the Nakamiro channel. In contrast, the maximum velocities are 0.5 m/s and 1.6 m/s, respectively. In addition, note that the flow and velocity is negative for a short period of time for the Lubigi channel.

The results also show a constant depth for both channels when a water level of 1.5 meters is reached. Additionally, for the Nakamiro channel, there is a constant flow of 16 m³/s and a constant velocity of 1.5 m/s.

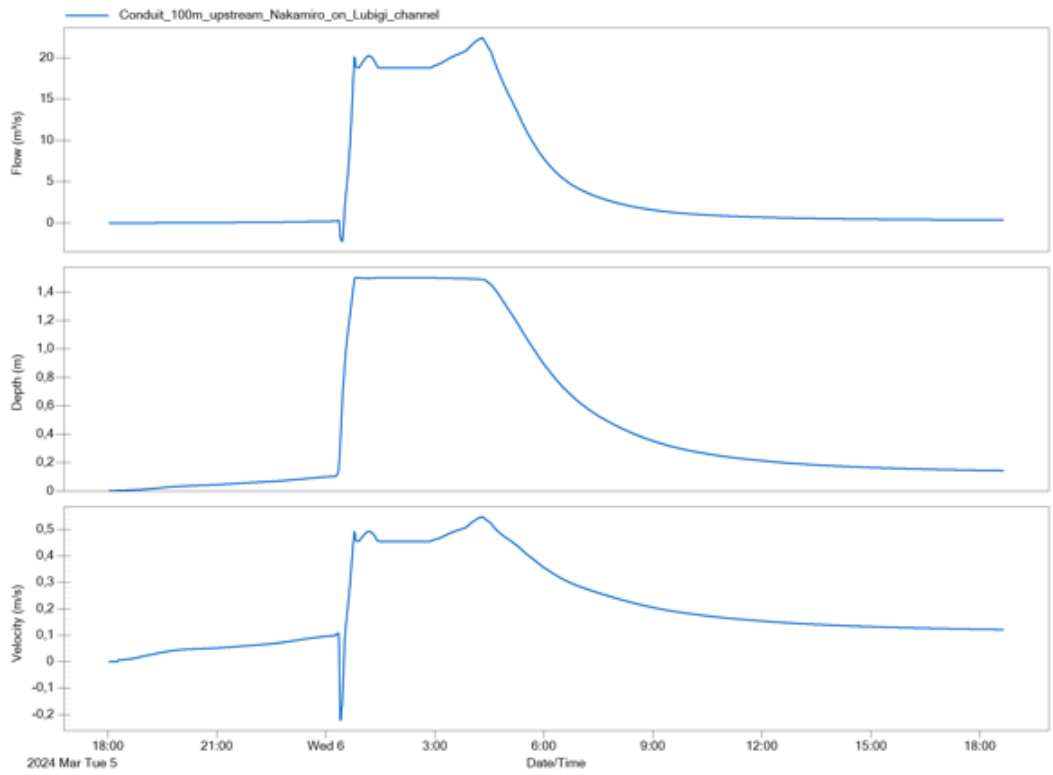

Figure 22 Flow, depth, and velocity hydrographs for location (1) upstream of the crossing on the Lubigi channel simulated with the 53.4 mm rain event on 06-03-2024.

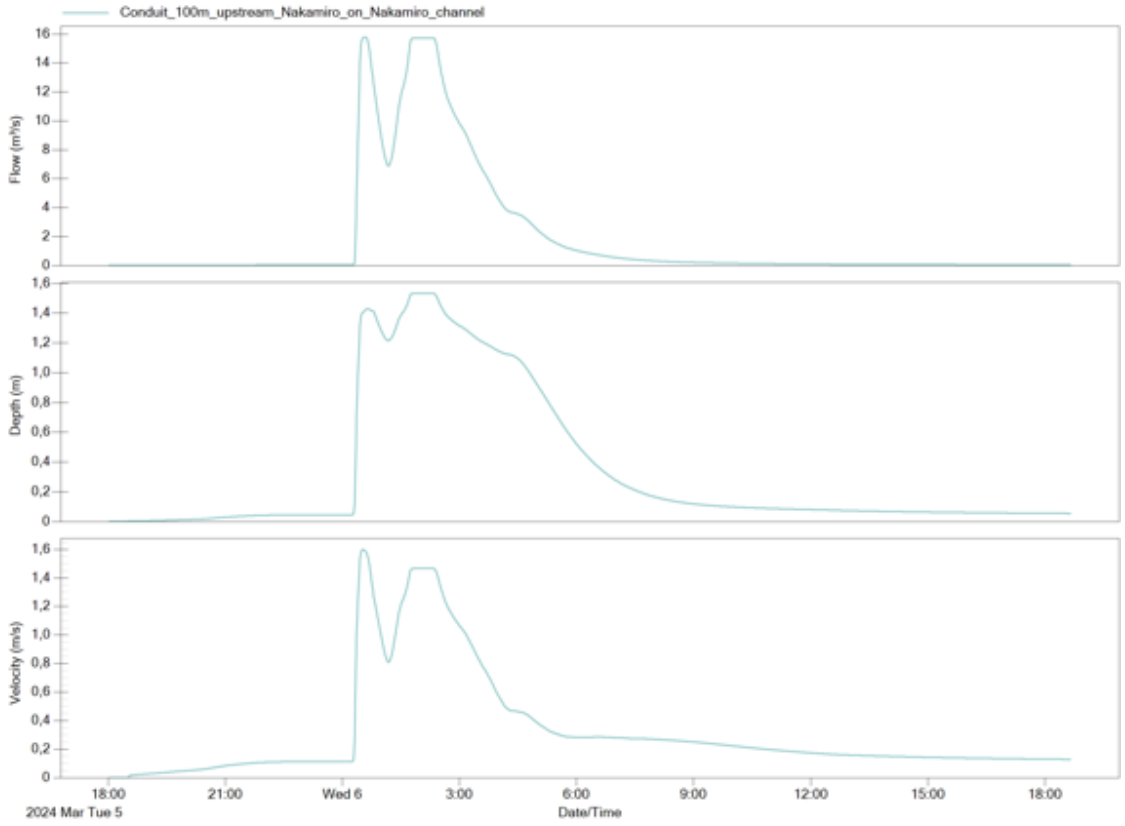

Figure 23 Flow, depth, and velocity hydrographs for location (2) upstream of the crossing on the Nakamiro channel, simulated with the 53.4 mm rain event on 06-03-2024.

Figure 24 shows the flow, depth, and velocity hydrographs for location (3) downstream the crossing. The flow, which is the resulting flow from location (1) and (2) is approximately 25 m^3/s. The depth is constant when a water level of 1.5 m is reached, in correlation with the depths in Figure 22 and Figure 23. Note that the velocity is negative for a short period of time.

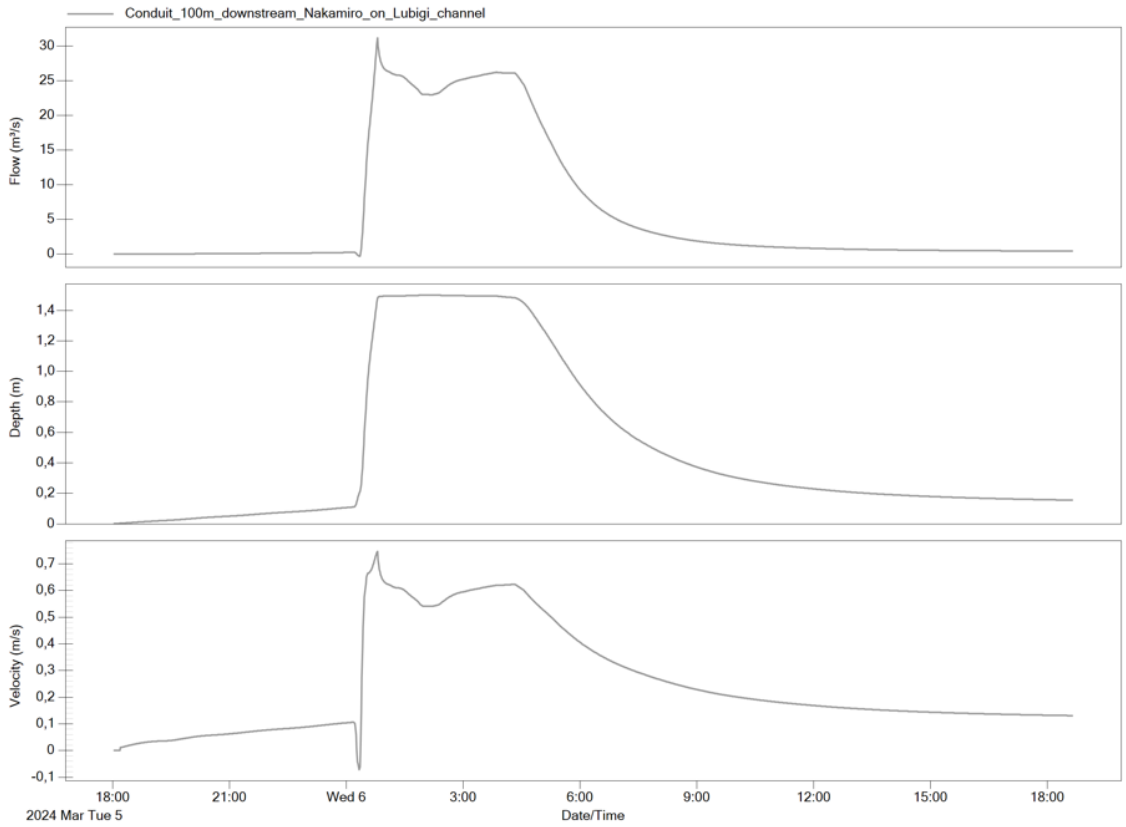

Figure 24 Flow, depth, and velocity for location (3) downstream the crossing.

4.2.2 Alice Kaggwa Road and Kamwokya Kisalosalo Road

Reviewing the flooding's at Alice Kaggwa Road and Kamwokya Kisalosalo Road reveals that undersized culverts may be a significant factor. The culvert crossings can be seen in Figure 25. Both locations contain circular culvert crossings. A diameter of 1 m per circular culvert were estimated in the field.

Figure 25 Culvert crossing at Alice Kaggwa Road (to the left) and Kamwokya Kisalosalo Road (to the right).

In Figure 26 and Figure 27, flow and depth hydrographs are shown before and after the culvert at Alice Kaggwa Road. The hydrographs show a decrease in both flow and depth after the culvert, which is likely due to the flooding occurring at the culvert's entrance.

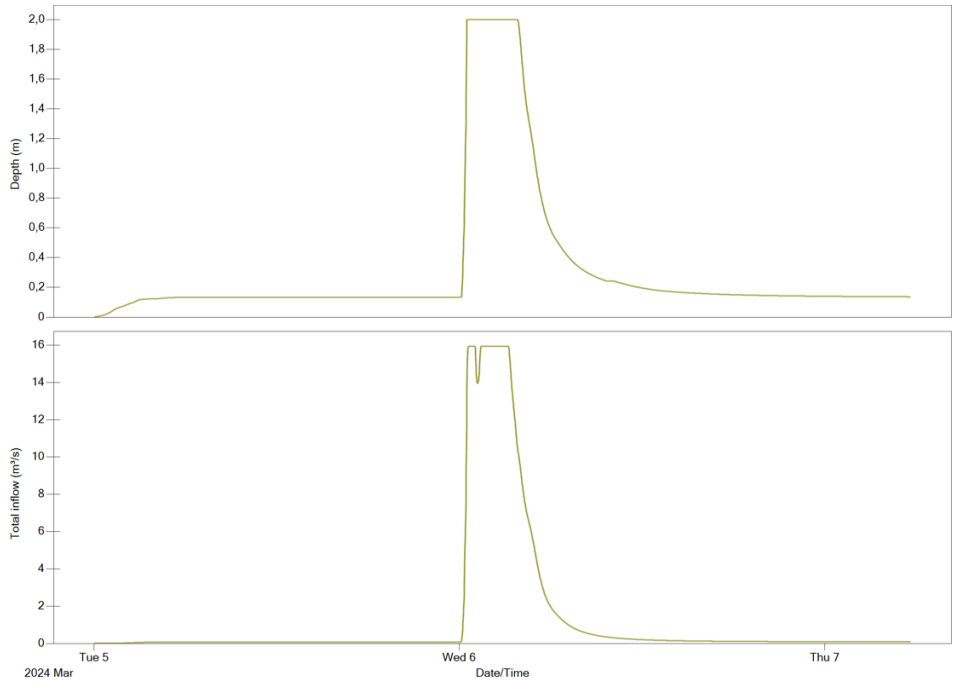

Figure 26 Flow and depth hydrographs at the opening of the culvert at Alice Kaggwa Road

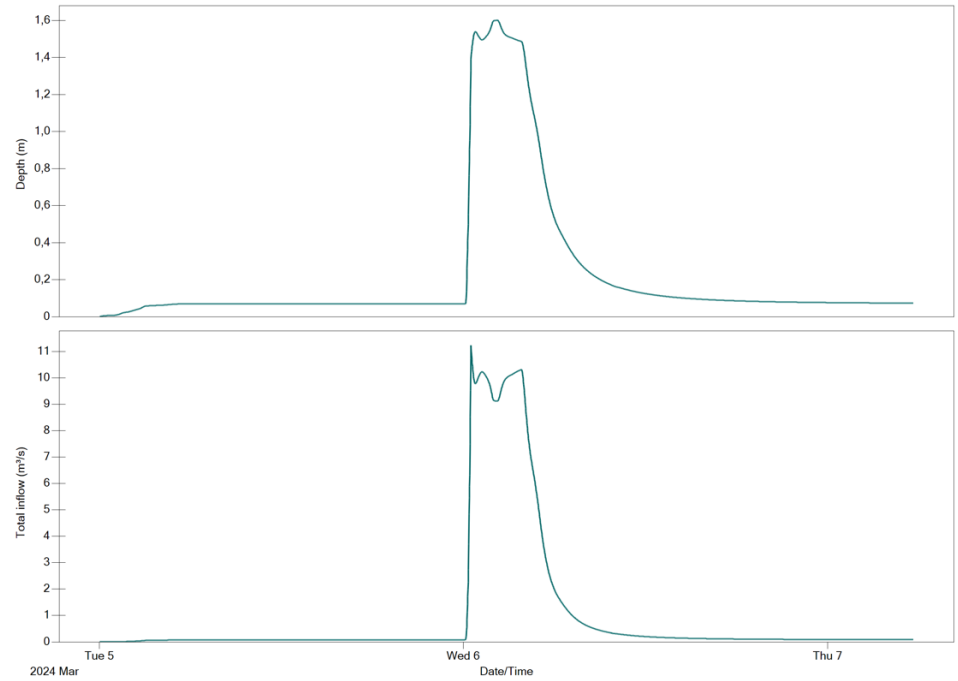

Figure 27 Flow and depth hydrographs at the end of the culvert at Alice Kaggwa Road.

In Figure 28 and Figure 29, flow and depth hydrographs are shown before and after the culvert at Kamwokya Kisalosalo Road. Like Alice Kaggwa Road, the hydrographs show a decrease in both flow and depth after the culvert. However, the reduction is significantly greater for Kamwokya Kisalosalo Road, with flow decreasing from approximately 25 m^3/s at the entrance to around 7,5 m^3/s at the exit. This corresponds to the larger flooding volume at Kamwokya Kisalosalo Road. Additionally, the culvert at Kamwokya Kisalosalo Road contains 3 circular culverts, compared to 4 circular culverts at Alice Kaggwa Road, which may explain the reason why the flow is reduced more at Kamwokya Kisalosalo Road than at Alice Kaggwa Road.

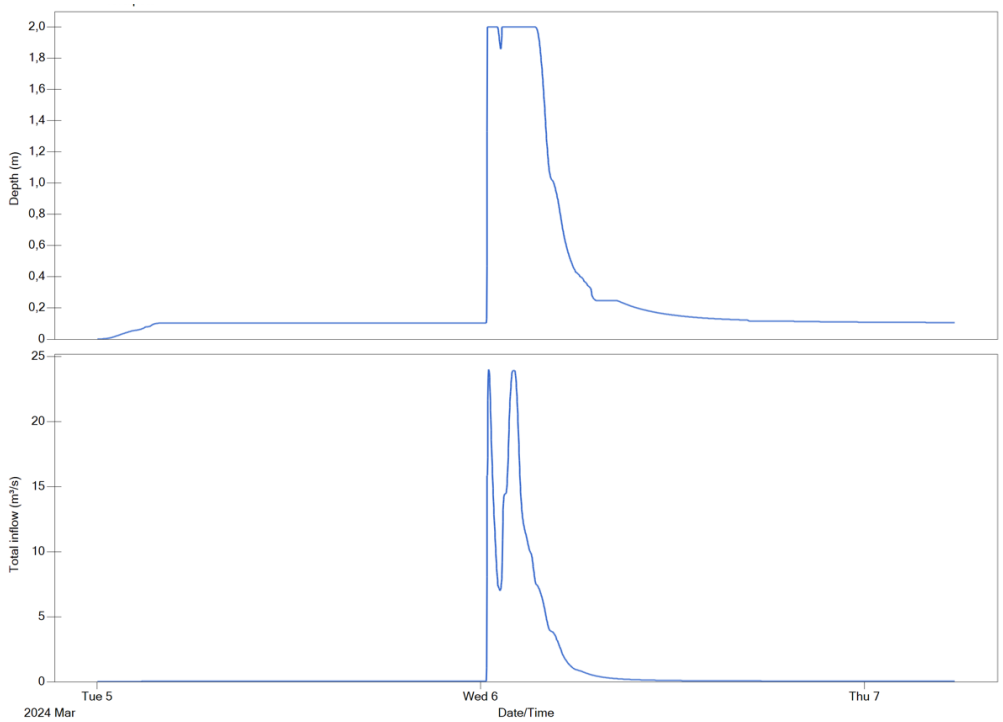

Figure 28 Flow and depth hydrographs at the opening of the culvert at Kamwokya Kisalosalo Road.

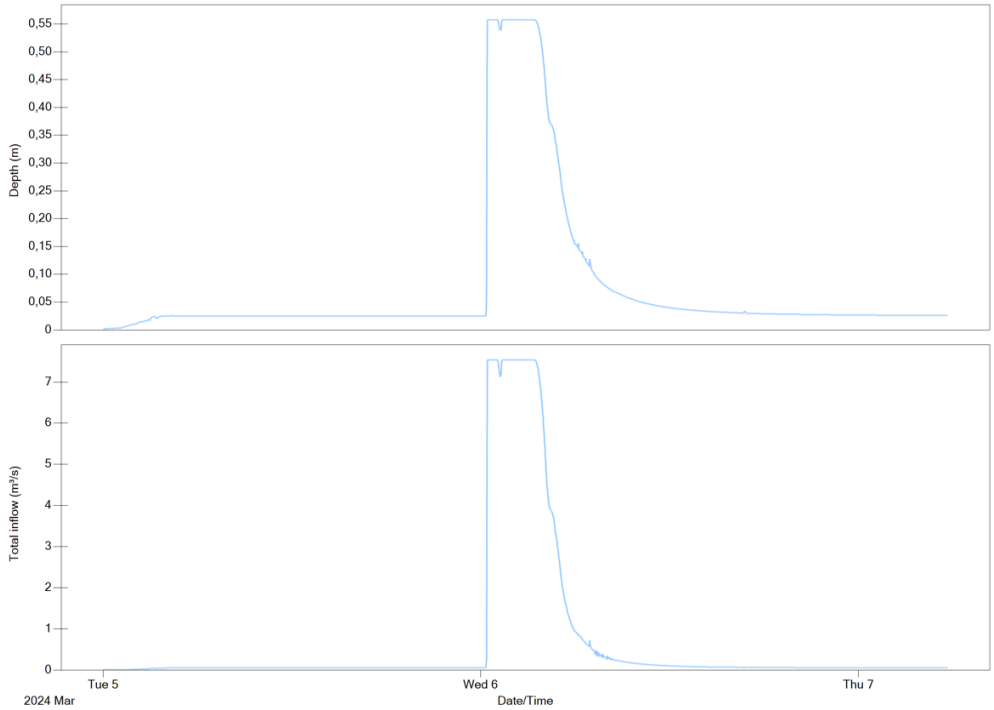

Figure 29 Flow and depth hydrographs at the end of the culvert at Kamwokya Kisalosalo Road

4.3 Scenario analysis

The following section describes the results of the scenario analysis. Table 3 show the results. The surface runoff and flooding volume that occurred in the additional sub catchments that include the wetland described as blue in Figure 12 is subtracted from the results to only visualize the volume of flooding in the main study area.

Flooding loss increases with increasing return period and sediment and solid waste deposition. The flooding loss percent, which describes the percentage of flooding loss relative to the surface runoff, also rises with increased sediment and solid waste deposition. Notably, the 52.6 mm rain event that occurred on 6 of March 2024, resulted in a higher percentage flooding loss than the T2 rain event across all scenarios, and almost equal the percentage of T10 for Scenario 3.

Flooding depth across the entire catchment area is calculated by dividing the flooding volume by the area of the whole catchment. This calculation provides a simplified visualization of flooding loss; however, it does not account for the uneven distribution of flooding due to variations in topography within the catchment, as illustrated in the table. In addition, the average runoff coefficient increases with increasing return period.

Table 3 Results from the scenario analysis including current scenario (1), 50% increase of sediment and solid waste at three locations (2) and 80% increase of sediment and solid waste at three locations (3). Note that the flooding indicators is highlighted in light grey and that the flooding depth is only used for reference.

Scenario 1 –Current sediment and solid waste deposition					
Rainfall	Average runoff coefficient (-)	Surface runoff (volume)	Flooding loss (volume)	Flooding loss (percent) *percent of surface runoff	Flooding depth across the entire catchment area
06-03-24	0.78	1 329 000 m^3	508 000 m^3	38 %	15 mm
T2	0.81	1 935 000 m^3	599 000 m^3	31 %	18 mm
T10	0.84	3 153 000 m^3	1 597 000 m^3	51 %	48 mm
T50	0.89	4 091 000 m^3	2 273 000 m^3	56 %	69 mm
T100	0.9	4 560 000 m^3	2 674 000 m^3	59 %	81 mm
Scenario 2 – 50 % Sediment and solid waste deposition					
06-03-24	0.78	1 329 000 m^3	658 000 m^3	50 %	20 mm
T2	0.81	1 935 000 m^3	757 000 m^3	39 %	23 mm
T10	0.84	3 153 000 m^3	1 732 000 m^3	55 %	52 mm
T50	0.89	4 091 000 m^3	2 538 000 m^3	62 %	77 mm
T100	0.9	4 560 000 m^3	2 951 000 m^3	65 %	89 mm
Scenario 3 – 80 % Sediment and solid waste deposition					
06-03-24	0.78	1 329 000 m^3	961 000 m^3	72 %	29 mm
T2	0.81	1 935 000 m^3	1 229 000 m^3	64 %	37 mm
T10	0.84	3 153 000 m^3	2 309 000 m^3	73 %	70 mm
T50	0.89	4 091 000 m^3	3 176 000 m^3	78 %	96 mm
T100	0.9	4 560 000 m^3	3 612 000 m^3	79 %	109 mm

5. Discussion

The following chapter discusses the results, following the same chronological order as the previous chapter is structured. Finally, it includes a comparison between the observed rainfall and the design storms used.

5.1 Model performance

As described in the result section, the validation resulted in acceptable NSE and RMSE values, indicating that the model can predict real-world conditions. However, since a model is a simplification of reality, the results should be interpreted with this in mind. The peak values used in the calibration and validation is based on water level indications on the culvert wall, which may contain uncertainties. Furthermore, the time of the peak is not accurately captured with this method. Installing an automatic water level meter in further research would capture the variations and peaks of the water levels better. In addition, performing flow measurements in the main channel would strengthen the model and could expand the range of modelling programs available, such as HEC-RAS, which relies on flow data as input for its simulations.

In the PCSWMM model developed, flooding loss is considered as water lost from the system, meaning the flooded water spreads over the ground surface and does not return. Although the “allow ponding” feature in PCSWMM could account for the flooded volume and was initially included in the modelling procedure, it was excluded due to unwanted results during the calibration.

As stated in the results, the wetland has been modelled in a simplified manner. Figure 19 indicates that the model may not accurately capture the flow in the wetland channel. This part was not modelled in detail because its location outside the boundaries of the upstream catchment and was included mainly to account for water backing up upstream. For example, secondary channels were not included here, the model only includes sub-catchments with direct inflow to the wetland channel, resulting in a contributing flow of 26.22 m^3/s, which could be an overestimation. This could explain the oscillating flow observed in Figure 19.

In addition, in the graph to the right in Figure 19, the flow contains multiple peaks which also occurs in the rest of the catchment. This could be explained by the timesteps used when interpreting the design rains in the model. By dividing the volumes in smaller time steps could possibly result in more smooth discharge curves that may represent actual rainstorms better.

For this master thesis project this were considered acceptable. Further research, by extending the area to include this would possibly make a more accurate model.

5.2 Critical points vulnerable to flooding

5.2.1 Bwaise

As described in the results, significant flooding is occurring at the Bwaise node. One possible explanation for this extensive flooding could be the *backwater effect* (Wang et al, 2019), which causes the upstream water level to rise, leading to flooding at the Bwaise node. The Nakamiro channel has a maximum flow of 16 m^3/s compared to 20 m^3/s in the upstream Lubigi channel, which could contribute to the backwater effect. Negative velocity can be seen in Figure 22 for location (1) and in Figure 24 for location (3). However, a negative velocity is not occurring at location (2), which could be an indication of a backwater effect. This effect could be analysed further by viewing the water level in the upstream location (1). However, the water level remains constant which could be due to the flooding.

On the contrary, a constant water depth is observed in all sections, with flooding occurring only at the Bwaise node. Another explanation for the constant water depths, might be due to the presence of box culverts, which is present upstream all these sections. To further analyse this, creating a 1D-2D model could potentially capture the water level variations better. However, the Digital Elevation Model (DEM) available for this catchment area was only available with a resolution of 30x30m, and there were high vertical differences compared to the invert levels used from KCCA. This discrepancy poses challenges in creating an accurate 1D-2D model.

Regardless of whether there is a backwater effect at the crossing, flooding is still occurring. To prevent this flooded volume from reaching the Northern Bypass, located south in Figure 21, and the adjacent residences, one solution could be to build flood walls. These walls could help direct the floodwater downstream.

5.2.2 Alice Kaggwa Road and Kamwokya Kisalosalo Road

Like in Bwaise, significant flooding also occurs at the circular culverts at Alice Kaggwa Road and Kamwokya Kisalosalo Road. A possible explanation for this could be that the culvert crossings are undersized for extreme rain events. It is important to note that the KCCA (2016) report described both crossings as box culverts, but on-site observations confirmed they are circular culverts (Figure 25). However, changing to box culverts at both locations would potentially reduce flooding at these locations.

5.3 Scenario Analysis

Table 3 include the results from the scenario analysis. Flooding loss in volume increases with both rain intensity and sediment and solid waste deposition. There is a noticeable change when comparing Scenario 3 with Scenario 1 and 2, particularly for the rain events with lower intensities (06-03-2024, T2). This indicates that maintaining the UDS should be prioritized not only to prevent flooding from rains with larger return periods but also from those with lower intensities.

By looking at the flooding depth at the entire catchment area, this is done for the reader to be able to visualize the flooding extent more easily. Only viewing volumes can be hard to grasp. It should be noted that this is not what would happen, water flows with decreasing elevation, which in this case is down to the main channel where it flows to the outfall. However, by looking at these values one can argue, especially for the rains with higher return periods (T10-T100), that this could possibly threaten communities, infrastructure, and the environment.

In Scenario 2 and 3, the excessive accumulation of sediment and solid waste is modelled by reducing the cross-sectional areas and adjusting the invert levels. While PCSWMM has a function to model the presence of sediment in pipes, it does not offer this capability for open channels. Therefore, only the cross-sectional areas were reduced. One could argue that the lack of tools for modelling sediment and solid waste in open channels is because this issue occurs more frequently in developing countries compared to developed countries. Highlighting this issue could hopefully lead to the inclusion of sediment and solid waste deposition for open channels in future updates of the modelling program.

In Scenario 1, which represent the current condition, this is modelled using a Manning's roughness coefficient for 0.05 for open channels containing sediment and solid waste and 0.1 for culvert crossings containing sediment and solid waste. It is challenging to determine if this accurately represent the existing condition. Other studies (Mugume et al., 2024) have modelled similar sediment and solid waste conditions using a lower bound of Manning's roughness coefficient equal 0.02, representing existing UDS without sediment (non-failed UDS), and an upper bound of Manning's roughness coefficient equal 100, representing partial or full structural failure (failed UDS) due to deposited sediment or solid waste.

In their study, they made a coupled 1D-2D model in the Nalukolongo and Kinawataka catchments in Kampala. The Nalukolongo catchment, which drains to the same receiving water body as the Lubigi catchment, consists of 1 primary channel and 8 secondary channels and has a similar catchment area as the upstream

part of Lubigi catchment studied in this thesis. They used the same derived IDF curves (Figure 15) but with a climate factor of 1.2, compared to 1.3 used in this study. However, their study did not include as detailed data for calibrating and validating the model as included in this master thesis project.

In Table 4, a comparison between the studies is shown. The model in the master thesis project simulates smaller flooding volumes for Scenario 1 compared to the non-failed scenario in Mugume et al. 2024, especially for smaller return periods. Scenario 3 shows similar flooding volumes when comparing the failed UDS in Mugume et al. 2024. However, decreasing the cross-sectional areas for simulating sediment and solid waste were not done in that study.

*Table 4 Comparison of flooding volumes between the master thesis and *(Mugume et al., 2024).*

Design storm	Scenario 1 Existing UDS (m^3)	Non-failed UDS* (m^3)	Difference in flooding volume	Scenario 3 80% sediment (m^3)	Failed UDS* (m^3)	Difference in flooding volume
T2	599 000	1 000 000	-40 %	1 229 000	1 200 000	+2%
T10	1 597 000	2 100 000	-24 %	2 309 000	2 500 000	-8%
T50	2 273 000	2 750 000	-17 %	3 176 000	3 100 000	+2%
T100	2 674 000	3 250 000	-18 %	3 612 000	3 500 000	+3%

With the above stated in mind, the flooding volumes calculated highlights the importance of restoring urban green areas, keeping the wetland undeveloped and finding solutions for keeping sediment and solid waste away from the channel. Combining BGI solutions (Mugume et al., 2024), in combination with sediment basin and silt fences (Prosser et al., 2001) could possibly be one way to go to reduce the flooding in the area.

5.4 Rainfall analysis

Comparing the high-resolution observed rainfall data from the tipping bucket rain gauge (Figure 7) with the design storms computed using the alternating block method from IDF curves for Kampala (Figure 16), reveals differences. For the observed rainfalls, the peak of the rainfall is occurring during the first 30 minutes for the two largest rainfalls recorded (6 of March 2024 and 23 of April 2024). However, for the design storms the peak is occurring after 120 minutes. This suggest that updating the design storms to have their peak occurring earlier in the rainfall event. This finding underscores the importance of installing additional rain gauges to obtain high-resolution rain data in developing countries, which is crucial for understanding and mitigating flooding.

6. Conclusions and Recommendations

In this chapter key conclusions are drawn based on the above results and discussion. After, recommendations are suggested based on the findings.

6.1 Conclusions

The main objective was to investigate how both current and increased sediment and solid waste deposits in the urban drainage system affect flooding within the upstream Lubigi catchment area. Additionally, the study aimed to identify critical points vulnerable to flooding, considering current sediment and solid waste deposits.

A 1D hydraulic model were developed in PCSWMM, including three scenarios describing the current, moderate, and severe accumulation of sediment and solid waste. The results show that the increasing sediment and solid waste deposition, increases the flooding in the catchment area. In addition, three critical points vulnerable to flooding were identified at Bwaise, Alice Kaggwa Road, and Kamwokya Kisalosalo Road. Lastly, the observed rainfalls from the installed tipping bucket rain gauge suggest that synthetic design storms in Kampala should include the rainfall peak earlier in the event than what is currently accounted for today.

Effective flood management in Kampala requires regular maintenance of urban drainage systems to prevent sediment and waste build-up. Additionally, integrating Blue-Green Infrastructure (BGI) and enhancing structural elements like culverts and flood walls are essential to improving the resilience of the drainage system.

The findings also highlight the broader implications of urbanization and climate change on flood risks, demanding a shift towards adaptive and sustainable flood management practices.

6.2 Recommendations

Future research should focus on several areas: refining sediment modelling techniques for open channels, conducting flow measurements to expand available data, exploring modelling tools like HEC-RAS, and, if high-resolution DEMs are available, develop a coupled 1D-2D model to better capture the complexities of urban flooding dynamics. To reduce the flooding in the upstream Lubigi catchment area, the following measures are recommended:

- Frequently clear sediment and solid waste from the main channel before it builds up, especially in the culvert crossings, it may need to be done more than two times a year, which is the frequency of today (H, Wasswa, personal communication, March 15, 2024).
- Identify if the channel in Lubigi wetland causes water to back up, leading to increased flooding upstream.
- Implement Blue-Green Infrastructure at various parts of the catchment. This could for example be to restore native vegetation along the main and secondary channels and keeping the wetland undeveloped.
- Look into the possibility to construct a flood wall to divert flow from the Nakamiro channel downstream and prevent flooding at Bwaise.
- Upscale the size of culvert crossings in the secondary channels, especially at Alice Kaggwa Road and Kamwokya Kisalosalo Road.
- Look into implementing sediment basins and silt fences to reduce sediment load in the primary and secondary channel.
- Consider updating current synthetic design storms for Kampala to include the rainfall peak earlier in the event.
- Enhance waste management practises to prevent solid waste from entering the urban drainage system.

References

Aksoy, H., Safari, M., Unal, N., Mohammadi, M. (2017). Velocity-based analysis of sediment incipient deposition in rigid boundary open channels. Water Sci Technol, 76 (9): 2535–2543. doi: https://doi.org/10.2166/wst.2017.429

Balbastre-Soldevila, R., García-Bartual, R., & Andrés-Doménech, I. (2019). A comparison of design storms for urban drainage system applications. Water (Switzerland), 11(4). https://doi.org/10.3390/w11040757

Barbosa A. E., Fernandes, J. N., & David, L. M. (2012). Key issues for sustainable urban stormwater management. Water research, 46(20), 6787-6798.

Basumatary, V., & Sil, B. S. (2017). Generation of Rainfall Intensity-Duration-Frequency curves for the Barak River Basin. Meteorology Hydrology and Water Management, 6(1), 47-57. https://doi.org/10.26491/mhwm/79175

Bohman, A., Glaas, E., & Karlson, M. (2020). Integrating sustainable stormwater management in urban planning: Ways forward towards institutional change and collaborative action. Water, 12(1), 203.

Butler, D., & Davies, J. W. (2011). Urban Drainage, 3rd Edition. Spon Press.

Chow, V. T., Maidment, D. R., & Mays, L. W. (1988). Applied Hydrology. McGraw-Hill.

Chang, N. B., Lu, J. W., Chui, T. F. M., & Hartshorn, N. (2018). Global policy analysis of low impact development for stormwater management in urban regions. Land use policy, 70, 368-383.

Chanson, H. (2004). Hydraulics of open channel flow (2nd ed.). Butterworth-Heinemann

Chereni, S., Sliuzas, R. V., Flacke, J., & Maarseveen, M. V. (2020). The influence of governance rearrangements on flood risk management in Kampala, Uganda. Environmental Policy and Governance, 30(3), 151-163.

Chitwatkulsiri, D., Miyamoto, H., Irvine, K. N., Pilailar, S., & Loc, H. H. (2022). Development and Application of a Real-Time Flood Forecasting System (RTFlood System) in a Tropical Urban Area: A Case Study of Ramkhamhaeng Polder, Bangkok, Thailand. Water (Switzerland), 14(10). https://doi.org/10.3390/w14101641

Costa, S., Peters, R., Martins, R., Postmes, L., Keizer, J. J., & Roebeling, P. (2021). Effectiveness of nature-based solutions on pluvial flood hazard mitigation: The case study of the city of Eindhoven (The Netherlands). Resources, 10(3), 24. https://doi.org/10.3390/resources10030024

Dietz, M. E. (2007). Low impact development practices: A review of current research and recommendations for future directions. Water, air, and soil pollution, 186, 351-363.

Edokpayi, J. N., Odiyo, J. O., & Durowoju, O. S. (2017). Impact of Wastewater on Surface Water Quality in Developing Countries: A Case Study of South Africa. In Water Quality. InTech. https://doi.org/10.5772/66561

Echendu, A. J. (2023). Human factors vs climate change; experts' view of drivers of flooding in Nigeria. Natural Hazards Research, 3(2), 240-246.

EPA (Environmental Protection Agency). (2024). Storm Water Management Model (SWMM). Retrieved 28 May 2024 from https://www.epa.gov/water-research/storm-water-management-model-swm

Falconer, R. H., Cobby, D., Smyth, P., Astle, G., Dent, J., & Golding, B. (2009). Pluvial flooding: new approaches in flood warning, mapping and risk management. Journal of Flood Risk Management, 2(3), 198-208.

Fletcher, T. D., Shuster, W., Hunt, W. F., Ashley, R., Butler, D., Arthur, S., Trowsdale, S., Barraud, S., Semadeni-Davies, A., Bertrand-Krajewski, J. L., Mikkelsen, P. S., Rivard, G., Uhl, M., Dagenais, D., & Viklander, M. (2015). SUDS, LID, BMPs, WSUD and more – The evolution and application of terminology surrounding urban drainage. Urban Water Journal, 12(7), 525–542. https://doi.org/10.1080/1573062X.2014.916314

Ghosh, S. N. (2014). Flood control and drainage engineering, fourth edition. CRC Press.

Haghighatafshar, S., Becker, P., Moddemeyer, S., Persson, A., Sörensen, J., Aspegren, H., & Jönsson, K. (2020). Paradigm shift in engineering of pluvial floods: From historical recurrence intervals to risk-based design for an uncertain future. Sustainable Cities and Society, 61. https://doi.org/10.1016/j.scs.2020.102317

Hellmers, S., Manojlović, N., Palmaricciotti, G., Kurzbach, S., & Fröhle, P. (2018). Multiple linked sustainable drainage systems in hydrological modelling for urban drainage and flood risk management. Journal of flood risk management, 11, S5-S16.

HOBO. (n.d.). HOBO Data Logging Rain Gauge (RG3 and RG3-M) Manual.

IPCC. (2023). Climate Change 2023: Synthesis Report. Contribution of Working Groups I, II and III to the Sixth Assessment Report of the Intergovernmental Panel on Climate Change, Geneva: IPCC.

IPCC. (2018). Summary for policymakers, in Global Warming of 1.5 °C. An IPCC Special Report on the Impacts of Global Warming of 1.5 °C Above Pre-Industrial Levels and Related Global Greenhouse Gas Emission Pathways in the Context of Strengthening the Global Response to the Threat of Climate Change, Sustainable Development, and Efforts to Eradicate Poverty, eds V. Masson-Delmotte, P. Zhai, H.-O. P?rtner, D. Roberts, J. Skea, P. R. Shukla, A. Pirani, W. Moufouma-Okia, C. P?an, R. Pidcock, S. Connors, J. B. R. Matthews, Y. Chen, X. Zhou, M. I. Gomis, E. Lonnoy, T. Maycock, M. Tignor, and T. Waterfield (Geneva: World Meteorological Organization), 32.

IPCC. (2007). Climate Change 2007: Synthesis Report. Contribution of Working Groups I, II and III to the Fourth Assessment Report of the Intergovernmental Panel on Climate Change IPCC, Geneva.

Jemberie, M. A., Melesse, A. M., & Abate, B. (2023). Urban Drainage: The Challenges and Failure Assessment Using AHP, Addis Ababa, Ethiopia. Water, 15(5), 957., https://www.mdpi.com/2073-4441/15/5/957

KCCA. (2020). Consultancy services for design review of drainage improvement works in Kampala (Lot 1 – Lubigi primary channel and Lot 2 – Nakamiro secondary channel)

KCCA. (2016). Kampala Drainage Master Plan 2016 Final Technical Report.

Kourtis, I. M., & Tsihrintzis, V. A. (2022). Update of intensity-duration-frequency (IDF) curves under climate change: a review. Water Supply, 22(5), 4951–4974. https://doi.org/10.2166/ws.2022.152

Koutsoyiannis, D., Kozonis, D., & Manetas, A. (1998). A mathematical framework for studying rainfall intensity-duration-frequency relationships. In Journal of Hydrology ELSEVIER Journal of Hydrology (Vol. 206).

Kozak, D., Henderson, H., de Castro Mazarro, A., Rotbart, D., & Aradas, R. (2020). Blue-green infrastructure (BGI) in dense urban watersheds. The case of the Medrano stream basin (MSB) in Buenos Aires. Sustainability, 12(6), 2163.

Lawhon, M., Ernstson, H., and Silver, J. (2014). Provincialising urban political ecology: towards a situated UPE through African urbanism. Antipode 46, 497–516. doi: 10.1111/anti.12051

Liao, K. H., Deng, S., & Tan, P. Y. (2017). Blue-Green Infrastructure: New Frontier for Sustainable Urban Stormwater Management. In Advances in 21st Century Human Settlements (pp. 203–226). Springer. https://doi.org/10.1007/978-981-10-4113-6_10

Lyn, D.A. Chen, W.F., Liew, R. (2003). Sediment Transport in Open Channels. In Chen, W.F., Liew, R. (Eds.), The Civil Engineering Handbook (2nd ed). CRC Press.

NatuReS. (n.d.). Partnership progress towards jointly tackling flooding in Greater Kampala. Retrieved from https://nature-stewardship.org/countries/uganda/progress-towards-jointly-tackling-flooding-in-kampala/

Niu, Z., Long, Y., Meng, C., Yang, H., Luo, Y., & Zhao, W. (2023). Impact Pressure Influence of Flood on Bridge Deck under Sediment Deposition Conditions: An Experimental Study. Sustainability, 15(18), 13778.

Nimusiima, A., Faridah, N., Isaac, M., Bob, A. O., & Peter, W. (2021). A community perspective of flood occurrence and weather forecasting over Kampala City. African Journal of Environmental Science and Technology, 15(5), 188–201. https://doi.org/10.5897/ajest2021.3007

Mahmood, A., Han, J. C., Ijaz, M. W., Siyal, A. A., Ahmad, M., & Yousaf, M. (2022). Impact of Sediment Deposition on Flood Carrying Capacity of an Alluvial Channel: A Case Study of the Lower Indus Basin. Water, 14(20), 3321.

Maksimović, Č., Prodanović, D., Boonya-Aroonnet, S., Leitão, J. P., Djordjević, S., & Allitt, R. (2009). Overland flow and pathway analysis for modelling of urban pluvial flooding. Journal of Hydraulic Research, 47(4), 512-523. https://doi.org/10.1080/00221686.2009.9522027

Mokuolu, J. O., Dauda, K. T., & Olajoke, A. K. (2022). Assessing the effects of solid wastes on urban flooding: A case study of Isale Koko. *LAUTECH Journal of Civil and Environmental Studies, 9*(1), 24-30.

Mugume, S. N., Kibibi, H., Sorensen, J., & Butler, D. (2024). Can Blue-Green Infrastructure enhance resilience in urban drainage systems during failure conditions? Water Science & Technology. https://doi.org/10.2166/wst.2024.032

Mugume, S. N., & Butler, D. (2017). Evaluation of functional resilience in urban drainage and flood management systems using a global analysis approach. Urban Water Journal, 14(7), 727–736. https://doi.org/10.1080/1573062X.2016.1253754

Mugume, S. N., Gomez, D., Melville-Shreeve, P., & Butler, D. (2017). Multifunctional urban flood resilience enhancement strategies. Proceedings of the Institution of Civil Engineers: Water Management, 170(3), 115–127. https://doi.org/10.1680/jwama.15.00078

Mugume, S. N., & Butler, D. (2015). Moving from reliability to resilience-based evaluation of urban drainage infrastructure: A case study of Kampala, Uganda. In Proceedings of the 10th International Urban Drainage Modelling Conference, Quebec, Canada, pp. 237–240.

Mugume, A., Mugume, S., Gomez, D., & Butler, D. (2015). Statistical methods for climate change impact assessment on urban rainfall extremes for cities in tropical developing countries – A review. In: International Conference on Flood Resilience: Experiences in Asia and Europe (Butler D., Chen A. S., Djordjevic S. & Hammond M. J., eds). University of Exeter, Exeter, United Kingdom.

Mugume, S. N. (2015). *Modelling and Resilience-based Evaluation of Urban Drainage and Flood Management Systems for Future Cities* [Doctoral dissertation, University of Exeter]. Open Research Exeter. https://ore.exeter.ac.uk/repository/bitstream/handle/10871/18870/MugumeS.pdf?sequence=4&isAllowed=y

Møller-Jensen, L., Agergaard, J., Andreasen, M. H., Kofie, R. Y., Yiran, G. A., and Oteng-Ababio, M. (2023). Probing political paradox: Urban expansion, floods risk vulnerability and social justice in urban Africa. J. Urban Aff. 45, 505–521. doi: 10.1080/07352166.2022.2108436

Oteng-Ababio, M., Agergaard, J., Møller-Jensen, L., & Andreasen, M. H. (2024). Flood risk reduction and resilient city growth in sub-Saharan Africa: searching for coherence in Accra's urban planning. Frontiers in Sustainable Cities, 6, 1118896.

Ortega Sandoval, A. D., Sörensen, J., Rodríguez, J. P., & Bharati, L. (2023). Hydrologic-hydraulic assessment of SUDS control capacity using different modeling approaches: a case study in Bogotá, Colombia. Water Science and Technology, 87(12), 3124–3145. https://doi.org/10.2166/wst.2023.173

Owusu, G., & Oteng-Ababio, M. (2015). Moving unruly contemporary urbanism toward sustainable urban development in Ghana by 2030. Am. Behav. Sci. 59, 311–327. doi: 10.1177/0002764214550302

Pérez-Molina, E., Sliuzas, R., Flacke, J., & Jetten, V. (2017). Developing a cellular automata model of urban growth to inform spatial policy for flood mitigation: A case study in Kampala, Uganda. Computers, environment and urban systems, 65, 53-65.

Poussin, J. K., Bubeck, P., Aerts, J. C. J. H., & Ward, P. J. (2012). Potential of semi-structural and non-structural adaptation strategies to reduce future flood risk: case study for the Meuse. Natural Hazards and Earth System Sciences, 12(11), 3455-3471.

Prosser, I. P., Rutherfurd, I. D., Olley, J. M., Young, W. J., Wallbrink, P. J., & Moran, C. J. (2001). Large-scale patterns of erosion and sediment transport in river networks, with examples from Australia. Marine and Freshwater Research, 52(1), 81-99.

Ritter, A., & Muñoz-Carpena, R. (2013). Performance evaluation of hydrological models: Statistical significance for reducing subjectivity in goodness-of-fit assessments. Journal of Hydrology, 480, 33–45. https://doi.org/10.1016/j.jhydrol.2012.12.004

Rossman, L., & Simon, M. (2022). Storm Water Management Model User's Manual Version 5.2. United States Environmental Protection Agency.

Schmitt, T.G., & Scheid, C. (2020). Evaluation and communication of pluvial flood risks in urban areas. Wiley Interdiscip. Rev. Water 7, 1–14. https://doi.org/10.1002/WAT2.1401

Sliuzas, R., Flacke, J., Jetten, V. (2013). Modelling Urbanization and Flooding in Kampala, Uganda. University of Twente.

Sohn, W., Kim, J-H., Li, M-H., Brown, R. D., Jaber, F. H. (2020). How does increasing impervious surfaces affect urban flooding in response to climate variability? Ecological indicators, 118. https://doi.org/10.1016/j.ecolind.2020.106774

Stevaux, J. C., Latrubesse, E. M., Hermann, M. L. de P., & Aquino, S. (2010). Floods in urban areas of Brazil. In J. C. Stevaux, E. M. Latrubesse, M. L. de P. Hermann, & S. Aquino (Eds.), *Developments in Earth Surface Processes* (Vol. 13, pp. 245-252). Elsevier. https://doi.org/10.1016/S0928-2025(08)10013-X

SWWA. (2016). P110 Drainage of runoff and wastewater - Functional requirements, hydraulic dimensioning and design of public sewer systems (in Swedish). Swedish Water and Wastewater Association (Svenskt Vatten).

Sörensen, J., & Emilsson, T. (2018). Evaluating flood risk reduction by urban blue-green infrastructure using insurance data. Journal of Water Resources Planning and Management 145 (2), 1–11. https://doi.org/10.1061/(ASCE)WR.1943-5452.0001037

Tang, H., McGuire, L. A., Kean, J. W., & Smith, J. B. (2020). The impact of sediment supply on the initiation and magnitude of runoff-generated debris flows. Geophysical Research Letters, 47(14), e2020GL087643.

UN (United Nations Department of Economic and Social Affairs). (2022). World's Population Prospects 2022 Summary of Results.

UN (United Nations Department of Economic and Social Affairs). (2018). Worlds Urbanisations Prospects 2018 Highlights.

UN (United Nations Department of Economic and Social Affairs, Population Division) (2015). World urbanization prospects: The 2014 revision.

UNDP (United Nations Development Programme). (2023). Identifying solutions to Uganda's flooding challenge through community engagement. Retrieved 20 April 2024 from https://www.undp.org/uganda/blog/identifying-solutions-ugandas-flooding-challenge-through-community-engagement

Wang, X., Yan, X., Duan, H., Liu, X., & Huang, E. (2019). Experimental study on the influence of river flow confluences on the open channel stage-discharge relationship. Hydrological Sciences Journal, 64(16), 2025–2039. https://doi.org/10.1080/02626667.2019.1661415

Xueqin, L., Lindsay, C., Stringer, M, Dallimer. (2022). The role of blue green infrastructure in the urban thermal environment across seasons and local climate zones in East Africa. Sustainable Cities and Society, Volume 80, 2022, 103798, ISSN 2210-6707, https://doi.org/10.1016/j.scs.2022.103798.

Yang, B., & Li, S. (2013). Green infrastructure design for stormwater runoff and water quality: Empirical evidence from large watershed-scale community developments. Water, 5(4), 2038-2057.

Yazdanfar, Z., & Sharma, A. (2015). Urban drainage system planning and design–challenges with climate change and urbanization: a review. Water Science and Technology, 72(2), 165-179.

Zambrano, L., Pacheco-Muñoz, R., & Fernández, T. (2018). Influence of solid waste and topography on urban floods: The case of Mexico City. *Ambio, 47*(7), 771-780. https://doi.org/10.1007/s13280-018-1023-1